Open access • Journal Article • DOI:10.1038/NI.3659

Postprandial macrophage-derived IL-1β stimulates insulin, and both synergistically promote glucose disposal and inflammation — Source link

Erez Dror, Elise Dalmas, Daniel T. Meier, Stephan Wueest ...+16 more authors

Institutions: University Hospital of Basel, Boston Children's Hospital, university of lille, University of Lausanne ...+1 more institutions

Published on: 01 Mar 2017 - Nature Immunology (Nature Research)

Topics: Insulin receptor, Insulin, Postprandial, Carbohydrate metabolism and Type 2 diabetes

Postprandial macrophage-derived IL-1 stimulates insulin, and both synergistically promote glucose disposal and inflammation

Dror, Erez ; Dalmas, Elise ; Meier, Daniel T ; Wueest, Stephan ; Thévenet, Julien ; Thienel, Constanze ; Timper, Katharina ; Nordmann, Thierry M ; Traub, Shuyang ; Schulze, Friederike ; Item, Flurin ; Vallois, David ; Pattou, Francois ; Kerr-Conte, Julie ; Lavallard, Vanessa ; Berney, Thierry ; Thorens, Bernard ; Konrad, Daniel ; Böni-Schnetzler, Marianne ; Donath, Marc Y

Abstract: The deleterious effect of chronic activation of the IL-1 system on type 2 diabetes and other metabolic diseases is well documented. However, a possible physiological role for IL-1 in glucose metabolism has remained unexplored. Here we found that feeding induced a physiological increase in the number of peritoneal macrophages that secreted IL-1 , in a glucose-dependent manner. Subsequently, IL-1 contributed to the postprandial stimulation of insulin secretion. Accordingly, lack of endogenous IL-1 signaling in mice during refeeding and obesity diminished the concentration of insulin in plasma. IL-1 and insulin increased the uptake of glucose into macrophages, and insulin reinforced a pro-inflammatory pattern via the insulin receptor, glucose metabolism, production of reactive oxygen species, and secretion of IL-1 mediated by the NLRP3 inflammasome. Postprandial inflammation might be limited by normalization of glycemia, since it was prevented by inhibition of the sodium-glucose cotransporter SGLT2. Our findings identify a physiological role for IL-1 and insulin in the regulation of both metabolism and immunity.

DOI: https://doi.org/10.1038/ni.3659

Postprandial macrophage-derived IL-1β stimulates insulin and both synergistically promote glucose disposal and inflammation

Erez Dror[1], Elise Dalmas[1,6], Daniel T. Meier[1,6], Stephan Wueest[2], Julien Thévenet[3], Constanze Thienel[1], Katharina Timper[1], Thierry M. Nordmann[1], Shuyang Traub[1], Friederike Schulze[1], Flurin Item[2], David Vallois[4], Francois Pattou[3], Julie Kerr-Conte[3], Vanessa Lavallard[5], Thierry Berney[5], Bernard Thorens[4], Daniel Konrad[2], Marianne Böni-Schnetzler[1,6], Marc Y. Donath[1,6]

[1]Clinic of Endocrinology, Diabetes and Metabolism University Hospital Basel, and Department Biomedicine, University of Basel, 4031 Basel, Switzerland

[2]Dept. of Pediatric Endocrinology and Diabetology and Children's Research Center University Children's Hospital, Steinwiesstrasse 75, 8032 Zurich, Switzerland

[3]University Lille, Inserm, CHU Lille, U1190 Translational research for diabetes, European Genomic Institute for Diabetes, EGID, 59000 Lille, France

[4]Center for Integrative Genomics, University of Lausanne, Lausanne, Switzerland

[5]Cell Isolation and Transplantation Center, Department of Surgery, Geneva University Hospitals and University of Geneva School of Medicine, 1211 Geneva, Switzerland

[6]Equal contribution

Correspondence: marc.donath@usb.ch

Abstract

The deleterious role of chronic activation of the IL-1β system in type 2 diabetes and other metabolic diseases is well documented. However, a possible physiological role of IL-1β in glucose metabolism remained unexplored. Here we show that feeding induces a physiological increase in the number of peritoneal macrophages, which secrete IL-1β in a glucose-dependent manner. Subsequently, IL-1β contributes to postprandial stimulation of insulin secretion. Accordingly, lack of endogenous IL-1β in mice during refeeding and obesity reduced plasma insulin. IL-1β and insulin increased glucose uptake into macrophages, and insulin reinforced a pro-inflammatory pattern via the insulin receptor, glucose metabolism, reactive oxygen species production, and NLRP3 inflammasome-mediated IL-1β secretion. Post-prandial inflammation is limited by normalization of glycemia and can be prevented by inhibition of sodium-glucose cotransporter 2 (SGLT2). Our findings identify a physiological role for IL-1β and insulin in the regulation of both metabolism and immunity.

Introduction

Activation of the innate immune system is an initial response of the body to infections and injuries. The resulting inflammation aims at protecting against stressors and at restoring tissue and organism homeostasis. This process is largely driven by IL-1β, one of the first described cytokines[1]. However, prolonged activation of the immune system by over-nutrition may eventually promote the development of metabolic diseases[2-6]. A critical sensor of nutrient overload is the NLRP3 inflammasome, which processes pro-IL-1β to its active form in various metabolic disorders. This is the case for uric acid crystals which activate the NLRP3 inflammasome in gout[7], for cholesterol crystals in atherogenesis[8], and for glucose, fatty acids and islet amyloid polypeptide in type 2 diabetes[9-13]. Importantly, a causal link between IL-1β-induced inflammation and these metabolic diseases has been demonstrated by various genetic and pharmacological approaches in animal models[14-16] and in clinical trials[17-21]. While these studies shed light on the pathological role of IL-1β in metabolism, a physiological function of IL-1β in metabolic control remains largely unexplored.

In response to pathogens and obesity, profound changes in the metabolism of immune cells take place[22-25]. Beyond supplying energy, nutrients can also act as signaling molecules that promote the activation of immune cells. Indeed, elevated glucose and other metabolites drive production of IL-1β by macrophages[14,26].

Insulin-producing β cells have the highest IL-1 receptor expression of any tissue[27] and the IL-1 receptor is the most abundantly expressed cell surface receptor on β cells[28], pointing to a hitherto unappreciated physiological function. While the deleterious role of high-dose and long-term IL-1β exposure on islet function and mass is well documented[29,30], a few mainly *in vitro* observations hint to a possible beneficial role of IL-1β in insulin secretion and β-cell survival[31,32].

Parenteral glucose stimulation leads to a rapid first and second phase of insulin release. In contrast, the physiological slower resorption of a meal elicits a sustained increase of insulin that depends on the duration of food intake[33]. Thereby the insulin response to enteral food intake cannot be solely accounted for by the associated changes in blood glucose. It is modulated by several insulin secretagogues including the incretin hormones GIP and GLP-1[34]. These hormones promote insulin secretion only when glucose levels are elevated. While GIP and GLP-1 are the best described incretins, other incretin-like factors are thought to exist.

Several studies show that food intake transiently induces a mild inflammatory response[35,36]. We hypothesized that IL-1β contributes to this postprandial inflammation, regulating whole body glucose homeostasis along with an innate immune response. Thereby, it may deliver the energy needed to activate the innate immune system in order to prevent the dissemination of microorganisms contained in the food. We show here that a postprandial rise in glucose leads to acute elevation of macrophage-derived IL-1β, which contributes to postprandial insulin secretion via the abundantly expressed IL-1 receptor on β cells. Insulin reinforces a pro-inflammatory state and stimulates macrophages to produce IL-1β via glucose metabolism, subsequent production of reactive oxygen species (ROS) which leads to activation of the inflammasome[14,37]. Both, insulin and IL-1β regulate glucose disposal, whereby IL-1β preferentially stimulates glucose uptake into the immune cell compartment.

Results

Feeding stimulates intra-peritoneal macrophages to produce IL-1β.

In order to study the physiological involvement of IL-1β in insulin secretion we performed overnight fasting followed by refeeding experiments in wild-type and *IL1b*$^{-/-}$ mice. Two hours after refeeding, circulating IL-1β concentration was increased in wild-type mice, while, as expected, IL-1β remained undetectable in *IL1b*$^{-/-}$ mice (**Fig. 1a**; for validation of the assay see **Supplementary Fig. 1a**). Of note, IL-1β concentration in serum was already elevated 30 minutes after refeeding (not shown). Next we investigated the source of increased IL-1β. Following refeeding, expression of *Il1b* mRNA and of the IL-1β-dependent chemokines *Cxcl1* and *Ccl2* were increased in the omental fat (the main site from which macrophages migrate into the peritoneum[38,39]; **Fig. 1b**) but not in the circulating leukocytes, liver, spleen, epididymal fat or subcutaneous fat (not shown). Furthermore, the number of stromal vascular cells isolated from the omentum was reduced (fasted: 41.8 ± 13.4 x 10^3 cells/mg; refed: 8.3 ± 2.6 x 10^3 cells/mg; mean ± s.e.m.). Accordingly, we observed a marked increase in the number of peritoneal cells (**Fig. 1c**), which displayed an increase in *Il1b* mRNA expression (**Fig. 1d**). Flow cytometry revealed that the majority of these cells were macrophages (**Fig. 1e**; for gating strategy see **Supplementary Fig. 1b**), a repartition that remained unchanged between fasting and refeeding (not shown). *Ex vivo*, spontaneous release of IL-1β by cultured peritoneal macrophages from fasted or refed mice was comparable (not shown). However, macrophages from refed mice released more IL-1β following stimulation with ATP (**Fig. 1f**). To validate the source of the increased IL-1β during refeeding, we generated *Il1b*$^{fl/fl}$*Lyz2*-Cre mice, which specifically lack IL-1β in the myeloid lineage (**Supplementary fig. 1c**). Two hours after refeeding, circulating IL-1β concentration was increased in wild-type mice but not in their *Il1b*$^{fl/fl}$*Lyz2*-Cre littermates (**Fig 1g**). We then tested whether the increase in serum glucose following feeding mediated the postprandial

increase in IL-1β. We treated mice with the SGLT2 inhibitor canagliflozin, which decreases glycemia via inhibition of renal glucose reabsorption. Treatment of mice with canagliflozin induced glycosuria and prevented postprandial increase in glucose and insulin (**Supplementary Fig. 1d-f**), along with a complete prevention of postprandial increase in circulating IL-1β (**Fig. 1h**). Similarly, injection of the non-metabolizable glucose analogue 2-deoxyglucose (2DG) prior to refeeding strongly reduced IL-1β release (**Fig. 1i**). Finally, we tested the role of bacterial products in the stimulation of postprandial IL-1β by treating mice with broad-spectrum antibiotics or lipopolysaccharide (LPS). Antibiotics-treated mice tended to have milder postprandial inflammation than untreated mice as detected by *Il1b* and *Cxcl1* gene expression in the omental fat pad (**Supplementary Fig. 1g, h**) together with a mild decrease in postprandial circulating IL-1β (**Supplementary Fig. 1i**) despite similar food intake and no change in the number of peritoneal cells (**Supplementary Fig. 1j-l**). *Ex vivo,* peritoneal macrophages from antibiotic-treated mice released less IL-1β, even in the presence of ATP (**Fig. 1j**). However, priming with LPS prior to ATP stimulation restored IL-1β secretion (**Fig. 1j**). Accordingly, *in vivo* i.p. injection of LPS into fed mice increased circulating IL-1β along with insulin and decreased blood glucose (**Fig. 1k**). However, injection of LPS in genomic *Il1b*$^{-/-}$ mice failed to induce insulin (**Fig. 1l**). This suggests that there is a need for a microbial-related stimulus and energy supply (glucose) to induce postprandial release of IL-1β. Thus, feeding increases the number of intra-peritoneal macrophages, which are primed by bacterial products to produce and release IL-1β in response to glucose.

Postprandial macrophage IL-1β promotes insulin secretion.

Next, we examined the direct effect of elevated IL-1β after refeeding on insulin secretion. First, we measured postprandial circulating insulin in littermate *Il1b*$^{-/-}$ or wild-type refed mice. *Il1b*$^{-/-}$ mice had reduced insulin secretion (**Fig. 2a**) and elevated blood glucose (**Supplementary Fig. 2a**) after refeeding compared to wild-type mice, despite comparable

food intake (not shown). Since the number of peritoneal cells was increased upon refeeding (**Fig. 1c**), and macrophages are the most abundant immune cells in the peritoneal cavity (**Fig. 1e**), we depleted macrophages in wild-type mice by i.p. injection of clodronate (**Supplementary Fig. 2b**) prior to performing fasting-refeeding experiments. Depletion of macrophages resulted in a marked decreased of postprandial insulin in the circulation (**Fig. 2b**). Similarly, postprandial insulin was lower in *Il1b*$^{fl/fl}$*Lyz2*-Cre mice compared to their wild-type littermates (**Fig. 2c**). In addition, acute blockade of IL-1 with its natural antagonist IL-1Ra prior to refeeding resulted in slightly decreased circulating insulin in wild-type mice (**Fig. 2d**) and elevated blood glucose (**Supplementary Fig. 2c**). Since obesity is associated with inflammation and chronically elevated IL-1β and insulin[9], we investigated the effect of acute (1 hour before refeeding) IL-1 antagonism in diet- induced obese (DIO) mice to substantiate the ability of endogenous IL-1β to regulate insulin. Blocking the elevated circulating levels of IL-1β (**Fig. 2e**) with IL-1Ra lowered fasting insulin levels in DIO mice (**Fig. 2f**) without changing insulin sensitivity or hepatic glucose production as determined by a hyperinsulinemic-euglycemic clamp (**Fig. 2g, h**). As a second model, genetically obese db/db mice were injected with IL-1Ra, which also decreased insulin levels (**Fig. 2i**). Therefore, postprandial IL-1β derived from myeloid cells promotes insulin secretion.

Acute exposure to IL-1β induces insulin secretion.

To directly test the effect of IL-1β on insulin secretion *in vivo*, we performed acute injections of IL-1β in mice followed by i.p. glucose tolerance test (GTT). IL-1β led to a marked elevation in insulin secretion (**Fig. 3a**) and improved glucose tolerance (**Fig. 3b**). Insulin was also increased and glycemia improved by IL-1β administration in the absence of a glucose bolus but to a much lesser extent (**Fig. 3c, d**; note the different scale in the y-axis compared to **3a & b**). This glucose-dependent potentiation of insulin secretion is reminiscent of effects elicited by the incretin hormones GLP-1 and GIP[34]. However, circulating active GLP-1

concentrations remained unchanged following IL-1β injections (**Supplementary Fig. 3a**). Furthermore, the effect of IL-1β on insulin secretion and glucose tolerance was identical in *Glp1r*$^{-/-}$/*Gipr*$^{-/-}$ double knock-out mice compared to their wild-type littermates (**Supplementary Fig. 3b, c**) and treatment of mice with the GLP-1 inhibitor Exendin fragment 9-39 did not reduce the IL-1β effect on insulin secretion (not shown). Therefore, IL-1β did not promote glucose-induced insulin secretion via incretin hormones. Since insulin secretion could be increased as a result of IL-1β-mediated peripheral insulin resistance, we determined if insulin sensitivity changes upon an acute IL-1β injection using insulin tolerance tests and hyperinsulinemic-euglycemic clamp studies. Acute injection of IL-1β had no effect on insulin sensitivity or hepatic glucose production (**Fig. 3e, Supplementary Fig. 3d**). IL-1β also improved glucose tolerance and strongly increased insulin secretion in DIO mice (**Fig. 3f, g**) and in genetically obese db/db mice (**Fig. 3h, i**). In contrast to wild-type mice, *interleukin 1 receptor-associated kinase 4* (*Irak4*$^{-/-}$) deficient mice injected with IL-1β before an i.p. GTT showed no improvement in insulin secretion and no change in glycemia (**Supplementary Fig. 3e, f**) demonstrating that the observed effects of IL-1β are mediated by the IL-1 receptor signal transduction pathways. Of note, i.p. injection of 0.1 g/kg of IL-1β resulted in circulating IL-1β concentrations similar to those obtained upon refeeding and also induced insulin secretion (**Fig. 3j, k**). Next we tested whether LPS has similar effects. Acute i.p. LPS injection improved glucose tolerance and increased insulin secretion in both wild-type and DIO mice (**Fig. 4a, b**). Importantly, IL-1Ra treatment blocked LPS-induced insulin secretion (**Fig. 4c**). Type 1 IL-1 receptor mRNA (*Il1r1*) was expressed at a much higher level in isolated endocrine cells than in islet resident immune or endothelial cells (**Fig. 4d**). Specific immunostaining of mouse pancreatic tissue sections revealed the presence of IL-1R1 in a subpopulation of β cells (**Fig. 4e**). Previous *in vitro* studies[32] demonstrated that very low concentrations of IL-1β increased glucose-stimulated insulin secretion from islets. We confirmed this effect in mouse and human islets, and with the human β-cell line ENDOC

(**Supplementary Fig. 3g-i**), suggesting a direct β-cell effect. To determine whether acute administration of IL-1β, *in vivo*, acts directly on the islet, we used streptozotocin (STZ) to eliminate β cells from recipient mice and transplanted them with islets from wild-type or *Il1r1*$^{-/-}$ donor mice. The effect of IL-1β on insulin secretion and glucose tolerance was lost in *Il1r1*$^{-/-}$ transplanted mice (**Fig. 4f, g**). These results suggest that systemic IL-1β potentiates glucose-induced insulin secretion via islet IL-1R1, and this is independent of the incretins GLP-1 and GIP or of changes in insulin resistance.

Insulin stimulates IL-1β secretion of macrophages

Since IL-1β enhanced insulin secretion during refeeding, we investigated the possible synergistic contribution of insulin and IL-1β to the stimulation of the immune system. First we investigated by flow cytometry the expression of the insulin receptor (InsR) on resident macrophages isolated from several tissues. We found that peritoneal macrophages had the highest insulin receptor expression compared to other resident macrophages (**Fig 5a**). Moreover, we found that the InsR was upregulated in peritoneal macrophages from DIO mice (**Fig. 5b**) and in the pro-inflammatory M1 compared to naive M0 macrophages, whereas it was mildly downregulated in anti-inflammatory M2 macrophages (**Fig. 5c, Supplementary Fig. 4a**). Accordingly, insulin induced AKT phosphorylation in naive M0, to a greater extent in M1 and not in M2 macrophages (**Fig. 5d, Supplementary Fig.4b**). The insulin effect on AKT phosphorylation was confirmed using a quantitative multiplex assay (**Fig. 5e**). In contrast to the PI3K activation pathway, insulin had no impact on MAPK signaling (**Fig. 5f**). Insulin also stimulated upregulation of the glucose transporter *Slc2a1* (encodes GLUT1, the isoform that is mainly expressed in immune cells[25]; **Fig. 5g**) and the expression of hexokinase 2 (*Hk2*), the rate-limiting enzyme in glycolysis (**Fig. 5h**), in M1 macrophages. In line with this pattern, a 2 hour insulin treatment increased glycolytic activity in M1 macrophages, but not in naive or M2 macrophages (**Fig. 5i, Supplementary**

Fig. 4c). In accordance with the phosphorylation assay, the AKT signaling inhibitor LY294002 but not the MAPK signaling inhibitor U0126 blocked the effect of insulin on glycolytic activity in M1 macrophages (**Fig. 5j**). Further, insulin induced glucose uptake in naive macrophages, and this effect was enhanced by IL-1β (**Fig 5k**). Similar to the pattern of insulin receptor expression and activation, insulin induced secretion of mature IL-1β preferentially in M1 macrophages in an NLRP3-dependent manner (**Fig. 6a**). Insulin also stimulated *Tnf*, *Il6*, and *Cxcl1* expression and protein release in M1 macrophages but independently of NLRP3 activation (**Supplementary Fig. 4d, e**). This insulin effect on IL-1β appeared to be independent of cell death and survival, which remained unaffected (**Supplementary Fig. 4f**). Similar to insulin-induced glycolysis, insulin stimulated IL-1β via the PI(3)K activation pathway and was blocked by LY294002 and downstream by the mTOR inhibitor rapamycin (**Fig. 6b**). We then tested the role of glucose metabolism in insulin-induced IL-1β secretion. First, the GLUT1 inhibitor fasentin blocked IL-1β secretion (**Fig. 6c**). In addition, insulin failed to induce IL-1β when cells were cultured with the non-metabolizable glucose analogue 2DG or with the mitochondria targeted ROS scavenger Mito-TEMPO (**Fig. 6d**). IL-1Ra was undetectable following short-term exposure (2 hours) to insulin (not shown) however prolonged (12 hours) exposure to insulin induced IL-1Ra in M0 and M1 macrophages indicating that the induction of IL-1β was later counterbalanced by IL-1Ra secretion (**Fig. 6e, f**). Similarly to our i*n vitro* data, acute injection of insulin in mice increased amounts of circulating IL-1β and CXCL1 (**Fig. 6g, Supplementary Fig. 4g**). Overall, these data show that insulin induces inflammasome-mediated IL-1β secretion via enhanced glucose metabolism and mitochondrial ROS production. These effects are dependent on the AKT/-PI(3)K pathway and on the activity status of the macrophages.

IL-1β shifts glucose uptake to immune cells

Next, we tested how IL-1β contributes to glucose disposal. Exposure of macrophages to IL-1β led to an increase in glucose uptake (**Fig. 7a**), while blocking endogenously produced IL-1 with IL-1Ra slightly decreased glucose uptake (**Fig. 7b**). We then examined the effect of IL-1β and insulin injection on glucose uptake in wild-type mice. To avoid glucose-stimulated insulin secretion, we only used trace amounts of non-metabolizable radiolabeled glucose. IL-1β stimulated glucose uptake in spleen and circulating leukocytes (**Fig. 7c, d**). IL-1β also increased glucose uptake in adipose tissue and in muscle, however to a lesser extent than insulin (**Fig. 7e-g**). This is potentially due to the mild stimulation of insulin secretion by IL-1β observed in the absence of a glucose bolus (**Fig. 3c**). To mimic the chronic elevation of IL-1β, we injected mice with IL-1β daily for 3 consecutive days and determined the number and glucose uptake of peritoneal cells. Similar to refed mice, IL-1β-injected mice had more peritoneal cells (**Fig. 7h**). *Ex vivo*, glucose uptake of macrophages from these mice was increased (**Fig. 7i**). To test the physiological relevance of IL-1β-induced glucose uptake, we investigated postprandial glucose uptake in immune cells of refed mice. Blockade of endogenous IL-1 with IL-1Ra decreased glucose uptake in peritoneal macrophages (**Fig. 7j**). To further examine the contribution of immune cells to overall body glucose disposal, we first used T and B cell deficient (*Rag2*$^{-/-}$) mice. A single injection of IL-1β prior to a GTT in *Rag2*$^{-/-}$ mice lowered glucose concentration as potently as in littermate control mice (**Supplementary Fig. 5a**). Since *Rag2*$^{-/-}$ mice have a compensatory increase in the number of macrophages, we additionally ablated macrophages in *Rag2*$^{-/-}$ mice with clodronate liposomes (**Supplementary Fig. 5b**). This diminished the profound beneficial effect of IL-1β on glucose disposal, despite increased insulin levels (**Fig. 7k**), suggesting that immune cells substantially contribute to IL-1β-induced glucose disposal. Thus, beside the stimulation of insulin, IL-1β directly regulates glycemia by promotion of glucose disposal preferentially in immune cells (**Supplementary Fig. 6**).

Discussion

In the present study we show that feeding induces a physiological elevation of macrophage-derived IL-1β that promotes postprandial insulin secretion. This effect depends on bacterial products, which primes macrophages to produce more pro-IL-1β, and on glucose that drives the maturation of IL-1β. The production of IL-1β by M1, and to a lesser extent by M0, macrophages is enhanced by insulin. Insulin upregulates functional insulin receptors, signaling via the AKT/-PI(3)K pathway, glucose uptake through the glucose transporter GLUT1, glucose metabolism, and ROS production that activates the NLRP3 inflammasome[14,37]. Both insulin and IL-1β regulate whole body glucose disposal by promoting glucose uptake in muscle and fat, and fuel the immune system by stimulating glucose uptake into the immune cell compartment. Ablation of macrophages in T- and B-cell deficient mice significantly reduced IL-1β-mediated glucose clearance. Self-amplification of the system is limited by normalization of glycemia.

The number of macrophages in the peritoneum was increased upon refeeding along with increased expression of inflammatory genes including *Il1b* in omental fat, which supports active trafficking of macrophages into the peritoneal cavity[40]. Therefore, feeding stimulates immune surveillance, possibly to limit the dissemination of microorganisms contained in food. Activation of the immune system requires energy and contributes substantially to whole-body glucose consumption. We provide evidence that both, bacterial products and glucose metabolism, are required to induce postprandial IL-1β secretion by peritoneal macrophages. Indeed, we show that peritoneal cells from refed mice have elevated *Il1b* mRNA levels. This might rather be promoted by translocation of ingested or intestinal bacterial products than by the microbiota itself[41-43], since pretreatment of mice with antibiotics before refeeding only mildly lowered IL-1β secretion. However, stimulation of IL-1β release strongly depends on glucose uptake and metabolism. Indeed, we observed that

decreasing glycemia via SGLT2 inhibition or blocking glycolysis with 2DG prevented postprandial IL-1β in the circulation. This suggests that from all factors that could mediate this effect during feeding, such as mechanical stress of the digestive system, fiber, amino acid and fat intake, it is mainly glucose that drives IL-1β secretion. Our results also suggest a role for insulin in postprandial IL-1β secretion since insulin increased glucose uptake and metabolism in macrophages. Inhibition of glucose uptake with fasentin or 2DG blocked insulin-induced IL-1β secretion. Downstream, inhibiting mitochondrial ROS production, which activates the NLRP3 inflammasome[14,37], also prevented insulin from inducing IL-1β.

Previous *in vitro* studies have shown that low concentrations of IL-1β mildly stimulate insulin secretion[32]. Here we show that *in vivo*, IL-1β injections strongly potentiate insulin secretion in the presence of a glucose bolus. However, the most natural way to stimulate insulin secretion is eating. We find that IL-1β-induced insulin release occurs in physiology by demonstrating that postprandially produced IL-1β increased insulin levels and decreased glycemia. This IL-1β effect is partly mediated by the highly expressed IL-1R1 on β-cells, since the effect of IL-1β on insulin secretion and glucose tolerance was blunted in diabetic mice transplanted with islets from *Il1r1*$^{-/-}$ mice.

The beneficial effects of postprandial IL-1β on glucose homeostasis are in apparent contrast to the glucose lowering effects of IL-1 antagonism in patients with type 2 diabetes[17] and to the well-described deleterious effects of IL-1β on islet function and survival[4]. Though IL-1β provokes β-cell demise[30,44], at low concentrations or upon short exposure, IL-1β paradoxically stimulates β-cell proliferation and decreases apoptosis[32]. Therefore, IL-1β is not only detrimental for β-cells but has more complex biological functions[45]. An explanation to reconcile the beneficial effects of IL-1 blockade in type 2 diabetes is the difference between acute and chronic effects and the concept of β-cell "rest". Indeed, potassium

channel openers, which decrease insulin secretion, ultimately improve insulin secretion in patients with type 2 diabetes[46]. The benefit of IL-1 antagonism in patients with type 2 diabetes could result from β-cell rest, possibly in combination with inhibition of the toxic effects of IL-1β.

A further explanation why chronic upregulation of IL-1β leading to elevated insulin levels may become unfavorable for metabolism stems from our observation that insulin reinforces the inflammatory state of macrophages through enhanced glucose uptake and metabolism and increased InsR expression in macrophages of DIO mice. Indeed, activated macrophages play a crucial role in insulin resistance[47]. In line with this, insulin receptor expression was also higher in macrophages from DIO mice, where macrophages have been shown to be pro-inflammatory[6]. Thus, we propose that insulin, which is increased in early stages of type 2 diabetes, may drive and sustain the inflammatory state in macrophages and may therefore contribute to the chronic low-grade inflammation associated with metabolic diseases. Thereby, TNFα, IL-6 and CXCL1 may also add to the effect of IL-1β. In support, myeloid cell-restricted InsR deficient mice are protected against metabolic inflammation and insulin resistance[48].

The effect of insulin in macrophages was previously studied without taking into account the polarization status of the macrophages [49]. Herein we show that insulin preferentially acts on pro-inflammatory M1 macrophages characterised by more InsRs, enhanced downstream AKT phosphorylation and glycolytic activity. Further insulin promotes the NLRP3 inflammasome and leads to macrophage-derived IL-1β release. Interestingly, peritoneal macrophages had the highest insulin receptor density, supporting their contribution to postprandial homeostasis.

343 SGLT2 inhibitors have recently been approved for the treatment of type 2 diabetes and the
344 EMPA-REG outcome study revealed an impressive reduction in mortality[50]. However the
345 mechanisms leading to this protective effect are unclear. In the present study, we show that
346 canagliflozin prevents postprandial IL-1β elevation in the circulation. This could be due to
347 increased glucose excretion in the urine, which prevents an overload of glucose in tissues,
348 thereby avoiding deleterious chronic effects of glucose-induced IL-1β.
349
350 Altogether, our findings show that IL-1β, a master regulator of inflammation, and insulin, a
351 key hormone in glucose metabolism, promote each other. Both have potent effects on
352 glucose homeostasis and on the activity of the immune system, supporting the emerging
353 concept that inflammatory mediators play a role not only in the pathology of metabolism
354 but are an integral part of its physiology. The physiological synergy between IL-1β and
355 insulin on glucose disposal may be required to cope with the concomitant challenge by
356 nutrients and microorganisms related to food intake.
357

Accession Codes

Not applicable

Data Availability Statement

The data that support the findings of this study are available from the corresponding author upon request.

Acknowledgments

This work was financially supported by the Swiss National Research Foundation (166519 to M.Y.D.) and the European Genomic Institute for Diabetes (ANR-10-LABX-46 to F.P.). We thank our technicians M. Borsigova, K. Dembinski and S. Haeuselmann for excellent technical assistance, S. Dimeloe, E. Traunecker, and D. Labes for technical advice, G. Bantug for technical and editorial advice, the center for transgenic models of the University of Basel and D. Klewe-Nebenius for supporting the production of the *Il1b*$^{fl/fl}$ mouse.

Author Contributions

E.Dr., M.B.S and M.Y.D designed the study and wrote the manuscript; E.Dr. performed and analyzed most of the experiments. M.B.S, E.Da, and D.T.M performed and analyzed experiments; C.T, K.T, T.N, S.T, F.S, and D.V helped with experiments. S.W, F.I, and D.K performed the clamps. J.T, F.P, J.K.C provided human islets and performed the islet transplantation experiments. V.L. and T.B provided human islets. B.T provided the *Gipr*$^{-/-}$ /*Glp1r*$^{-/-}$ mice; all co-authors helped with the manuscript. M.Y.D and M.B.S supervised the Research.

Competing Financial Interests Statement

M.Y.D. is listed as the inventor on a patent filed in 2003 for the use of an interleukin-1 receptor antagonist for the treatment of, or prophylaxis against, type 2 diabetes

385 **References**

386 1. Dinarello, C.A. Multiple biological properties of recombinant human interleukin 1
387 (beta). *Immunobiology* **172**, 301-315 (1986).

388 2. Wellen, K.E. & Hotamisligil, G.S. Inflammation, stress, and diabetes. *The Journal of*
389 *clinical investigation* **115**, 1111-1119 (2005).

390 3. Hotamisligil, G.S., Shargill, N.S. & Spiegelman, B.M. Adipose expression of tumor
391 necrosis factor-alpha: direct role in obesity-linked insulin resistance. *Science* **259**, 87-
392 91 (1993).

393 4. Donath, M.Y., Dalmas, E., Sauter, N.S. & Boni-Schnetzler, M. Inflammation in obesity
394 and diabetes: islet dysfunction and therapeutic opportunity. *Cell metabolism* **17**,
395 860-872 (2013).

396 5. Ehses, J.A., Boni-Schnetzler, M., Faulenbach, M. & Donath, M.Y. Macrophages,
397 cytokines and beta-cell death in Type 2 diabetes. *Biochemical Society transactions*
398 **36**, 340-342 (2008).

399 6. Donath, M.Y. & Shoelson, S.E. Type 2 diabetes as an inflammatory disease. *Nature*
400 *reviews. Immunology* **11**, 98-107 (2011).

401 7. Martinon, F., Petrilli, V., Mayor, A., Tardivel, A. & Tschopp, J. Gout-associated uric
402 acid crystals activate the NALP3 inflammasome. *Nature* **440**, 237-241 (2006).

403 8. Duewell, P*., et al.* NLRP3 inflammasomes are required for atherogenesis and
404 activated by cholesterol crystals. *Nature* **464**, 1357-1361 (2010).

405 9. Vandanmagsar, B*., et al.* The NLRP3 inflammasome instigates obesity-induced
406 inflammation and insulin resistance. *Nature medicine* **17**, 179-188 (2011).

407 10. Wen, H*., et al.* Fatty acid-induced NLRP3-ASC inflammasome activation interferes
408 with insulin signaling. *Nature immunology* **12**, 408-415 (2011).

409 11. Stienstra, R*., et al.* The inflammasome-mediated caspase-1 activation controls
410 adipocyte differentiation and insulin sensitivity. *Cell metabolism* **12**, 593-605 (2010).

12. Maedler, K.*, et al.* Glucose-induced beta cell production of IL-1beta contributes to glucotoxicity in human pancreatic islets. *The Journal of clinical investigation* **110**, 851-860 (2002).

13. Masters, S.L.*, et al.* Activation of the NLRP3 inflammasome by islet amyloid polypeptide provides a mechanism for enhanced IL-1beta in type 2 diabetes. *Nature immunology* **11**, 897-904 (2010).

14. Zhou, R., Tardivel, A., Thorens, B., Choi, I. & Tschopp, J. Thioredoxin-interacting protein links oxidative stress to inflammasome activation. *Nature immunology* **11**, 136-140 (2010).

15. Stienstra, R.*, et al.* Inflammasome is a central player in the induction of obesity and insulin resistance. *Proceedings of the National Academy of Sciences of the United States of America* **108**, 15324-15329 (2011).

16. Ehses, J.A.*, et al.* IL-1 antagonism reduces hyperglycemia and tissue inflammation in the type 2 diabetic GK rat. *Proceedings of the National Academy of Sciences of the United States of America* **106**, 13998-14003 (2009).

17. Larsen, C.M.*, et al.* Interleukin-1-receptor antagonist in type 2 diabetes mellitus. *The New England journal of medicine* **356**, 1517-1526 (2007).

18. van Asseldonk, E.J.*, et al.* Treatment with Anakinra improves disposition index but not insulin sensitivity in nondiabetic subjects with the metabolic syndrome: a randomized, double-blind, placebo-controlled study. *The Journal of clinical endocrinology and metabolism* **96**, 2119-2126 (2011).

19. Cavelti-Weder, C.*, et al.* Effects of gevokizumab on glycemia and inflammatory markers in type 2 diabetes. *Diabetes care* **35**, 1654-1662 (2012).

20. Hensen, J., Howard, C.P., Walter, V. & Thuren, T. Impact of interleukin-1beta antibody (canakinumab) on glycaemic indicators in patients with type 2 diabetes

mellitus: results of secondary endpoints from a randomized, placebo-controlled trial. *Diabetes & metabolism* **39**, 524-531 (2013).

21. Sloan-Lancaster, J*., et al.* Double-blind, randomized study evaluating the glycemic and anti-inflammatory effects of subcutaneous LY2189102, a neutralizing IL-1beta antibody, in patients with type 2 diabetes. *Diabetes care* **36**, 2239-2246 (2013).

22. Gubser, P.M*., et al.* Rapid effector function of memory CD8+ T cells requires an immediate-early glycolytic switch. *Nature immunology* **14**, 1064-1072 (2013).

23. Fox, C.J., Hammerman, P.S. & Thompson, C.B. Fuel feeds function: energy metabolism and the T-cell response. *Nature reviews. Immunology* **5**, 844-852 (2005).

24. Macintyre, A.N*., et al.* The glucose transporter Glut1 is selectively essential for CD4 T cell activation and effector function. *Cell metabolism* **20**, 61-72 (2014).

25. Freemerman, A.J*., et al.* Metabolic reprogramming of macrophages: glucose transporter 1 (GLUT1)-mediated glucose metabolism drives a proinflammatory phenotype. *The Journal of biological chemistry* **289**, 7884-7896 (2014).

26. Tannahill, G.M*., et al.* Succinate is an inflammatory signal that induces IL-1beta through HIF-1alpha. *Nature* **496**, 238-242 (2013).

27. Boni-Schnetzler, M*., et al.* Free fatty acids induce a proinflammatory response in islets via the abundantly expressed interleukin-1 receptor I. *Endocrinology* **150**, 5218-5229 (2009).

28. Benner, C*., et al.* The transcriptional landscape of mouse beta cells compared to human beta cells reveals notable species differences in long non-coding RNA and protein-coding gene expression. *BMC genomics* **15**, 620 (2014).

29. Bendtzen, K*., et al.* Cytotoxicity of human pI 7 interleukin-1 for pancreatic islets of Langerhans. *Science* **232**, 1545-1547 (1986).

30. Mandrup-Poulsen, T*., et al.* Affinity-purified human interleukin I is cytotoxic to isolated islets of Langerhans. *Diabetologia* **29**, 63-67 (1986).

31. Zawalich, W.S. & Zawalich, K.C. Interleukin 1 is a potent stimulator of islet insulin secretion and phosphoinositide hydrolysis. *The American journal of physiology* **256**, E19-24 (1989).

32. Donath, M.Y., Boni-Schnetzler, M., Ellingsgaard, H., Halban, P.A. & Ehses, J.A. Cytokine production by islets in health and diabetes: cellular origin, regulation and function. *Trends in endocrinology and metabolism: TEM* **21**, 261-267 (2010).

33. Caumo, A. & Luzi, L. First-phase insulin secretion: does it exist in real life? Considerations on shape and function. *American journal of physiology. Endocrinology and metabolism* **287**, E371-385 (2004).

34. Baggio, L.L. & Drucker, D.J. Biology of incretins: GLP-1 and GIP. *Gastroenterology* **132**, 2131-2157 (2007).

35. Van Oostrom, A.J., Sijmonsma, T.P., Rabelink, T.J., Van Asbeck, B.S. & Cabezas, M.C. Postprandial leukocyte increase in healthy subjects. *Metabolism: clinical and experimental* **52**, 199-202 (2003).

36. Herieka, M. & Erridge, C. High-fat meal induced postprandial inflammation. *Molecular nutrition & food research* **58**, 136-146 (2014).

37. Petrilli, V.*, et al.* Activation of the NALP3 inflammasome is triggered by low intracellular potassium concentration. *Cell death and differentiation* **14**, 1583-1589 (2007).

38. Okabe, Y. & Medzhitov, R. Tissue-specific signals control reversible program of localization and functional polarization of macrophages. *Cell* **157**, 832-844 (2014).

39. Platell, C., Cooper, D., Papadimitriou, J.M. & Hall, J.C. The omentum. *World journal of gastroenterology : WJG* **6**, 169-176 (2000).

40. Shrivastava, P. & Bhatia, M. Essential role of monocytes and macrophages in the progression of acute pancreatitis. *World journal of gastroenterology : WJG* **16**, 3995-4002 (2010).

41. Cani, P.D*., et al.* Metabolic endotoxemia initiates obesity and insulin resistance. *Diabetes* **56**, 1761-1772 (2007).

42. Breton, J*., et al.* Gut Commensal E. coli Proteins Activate Host Satiety Pathways following Nutrient-Induced Bacterial Growth. *Cell metabolism* **23**, 324-334 (2016).

43. Zhang, D*., et al.* Neutrophil ageing is regulated by the microbiome. *Nature* **525**, 528-532 (2015).

44. Corbett, J.A., Wang, J.L., Sweetland, M.A., Lancaster, J.R., Jr. & McDaniel, M.L. Interleukin 1 beta induces the formation of nitric oxide by beta-cells purified from rodent islets of Langerhans. Evidence for the beta-cell as a source and site of action of nitric oxide. *The Journal of clinical investigation* **90**, 2384-2391 (1992).

45. Hajmrle, C*., et al.* Interleukin-1 signaling contributes to acute islet compensation. *JCI insight* **1**, e86055 (2016).

46. Greenwood, R.H., Mahler, R.F. & Hales, C.N. Improvement in insulin secretion in diabetes after diazoxide. *Lancet* **1**, 444-447 (1976).

47. Olefsky, J.M. & Glass, C.K. Macrophages, inflammation, and insulin resistance. *Annual review of physiology* **72**, 219-246 (2010).

48. Mauer, J*., et al.* Myeloid cell-restricted insulin receptor deficiency protects against obesity-induced inflammation and systemic insulin resistance. *PLoS genetics* **6**, e1000938 (2010).

49. Costa Rosa, L.F., Safi, D.A., Cury, Y. & Curi, R. The effect of insulin on macrophage metabolism and function. *Cell biochemistry and function* **14**, 33-42 (1996).

50. Zinman, B*., et al.* Empagliflozin, Cardiovascular Outcomes, and Mortality in Type 2 Diabetes. *The New England journal of medicine* **373**, 2117-2128 (2015).

Figure legends

Figure 1

Feeding stimulates intra-peritoneal macrophages to produce IL-1β.

(**a**) Circulating IL-1β in wild-type (WT; n=22, 4 experiments) or *Il1b*$^{-/-}$ (n=3) mice before and after feeding (LLOD denotes the lowest level of detection). (**b**) Gene expression in omental fat isolated from fasted and refed mice (n=8, 3 experiments). (**c**) Number of peritoneal cells isolated per mouse (WT, fasted n=15 and refed n=17, 4 experiments). (**d**) *Il1b* gene expression in peritoneal cells isolated from fasted and refed mice (n=6). (**e**) Peritoneal cell composition following feeding determined by flow cytometry (pool of 4 refed mice). (**f**) IL-1β release of macrophages isolated from fasted (n=5) or refed (n=6) mice and stimulated with ATP. (**g-i**) Circulating IL-1β levels before (fasted) or after refeeding (refed) in *Il1b*$^{fl/fl}$*Lyz2*-Cre and WT mice (**g**; n=16 and 15, respectively), in mice treated with or without the SGLT2 inhibitor canagliflozin (**h**; n=13 per group), and in mice treated with or without 2DG (**i**; saline n=9, 2DG n=10). (**j**) *Ex vivo* IL-1β secretion in unstimulated (basal) macrophages isolated from refed mice pretreated for a week with or without antibiotics (ABX, left) or stimulated with ATP (middle) alone or following LPS priming (right). (**k**) Circulating IL-1β, insulin, and blood glucose levels after intra-peritoneal (i.p.) injection of LPS (1 mg/kg) in fed mice (n=8). (**l**) Circulating insulin levels in fed WT or *Il1b*$^{-/-}$ mice after i.p. injection of 1 mg/kg LPS or saline (WT; saline n=5, LPS n=7, *Il1b*$^{-/-}$; n=7). **P* < 0.05, ***P* < 0.01, ***P<0.001, ****P < 0.0001. Statistical significance (*P*) was determined by Student's t test and in (b, g, h, I) by ANOVA. All error bars denote s.e.m.

Figure 2

Postprandial macrophage-derived IL-1β promotes insulin secretion.

(**a**) Circulating insulin concentration before (fasted) or after refeeding (refed) in *Il1b*$^{-/-}$ or WT mice (n=6 and 11, respectively). (**b, c**) Circulating insulin before (fasted) or after refeeding (refed) in (**b**) WT mice injected with liposomes containing clodronate or PBS (n=17 per group; 3 experiments), and in (**c**) *Il1b*$^{fl/fl}$*Lyz2*-Cre (n=16) and WT (n=15) mice. (**d**) Circulating insulin following an acute injection of saline or 10 mg/kg IL-1Ra in refed WT mice (n=26 and 23, respectively). (**e**) Basal circulating IL-1β levels in control (n=8) or DIO (n=10) mice. (**f**) Circulating insulin following acute injections of saline or 10 mg/kg IL-1Ra in DIO mice (n=15 and 13 respectively). Hyperinsulinemic-euglycemic clamp in DIO mice pre-injected with saline or with 10 mg/kg IL-1Ra (n=4 and 5, respectively): (**g**) Glucose infusion rate, (**h**) hepatic glucose production. (**i**) Circulating insulin levels following acute injections of saline or 10 mg/kg IL-1Ra in db/db mice (n=4 and 5, respectively). **P* < 0.05, ***P* < 0.01. Statistical significance (*P*) was determined by Student's t test and in (a-c) by ANOVA. All error bars denote s.e.m.

Figure 3

Acute exposure to IL-1β induces insulin secretion without changing insulin sensitivity.

(**a, b**) Concentrations of circulating insulin (**a**) and glucose (**b**) during an intra-peritoneal glucose tolerance test (i.p. GTT) in WT mice 18 minutes after a single injection with saline or 1 μg/kg IL-1β (n=5 and 6, respectively). (**c, d**) Concentrations of circulating insulin (**c**) and glucose (**d**) in 6 hour fasted WT mice injected with or without 1 μg/kg IL-1β (n=8 per group). (**e**) Glucose infusion rate and hepatic glucose production during a hyperinsulinemic-euglycemic clamp in WT mice pre-treated with 1 μg/kg IL-1β or saline (n=4 and 3, respectively). (**f-i**) Concentrations of insulin (**f, h**) and glucose (**g, i**) during an i.p. GTT in diet-induced obese (DIO) (**f, g**) and db/db (**h, i**) mice, pre-treated with 1 μg/kg IL-1β (n=12 per group). (**j**) Circulating IL-1β concentration and (**k**) insulin (fold of basal) 18 min after an i.p. injection of 0.1 or 1 μg/kg of IL-1β into WT mice (n=9). **P* < 0.05, ***P* < 0.01, ***P<0.001,

563 ****P < 0.0001. Statistical significance (P) was determined by Student's t test and in (**k**) by
564 ANOVA. All error bars denote s.e.m.
565
566 **Figure 4**
567 **Systemic IL-1β potentiates glucose-induced insulin secretion via islet IL-1R1**
568 (**a**) Circulating insulin and (**b**) glucose levels during an i.p. GTT in WT and DIO mice 3 hours
569 after a single injection of LPS (1 mg/kg) or saline (n=5 per group). (**c**) Circulating insulin
570 during an i.p. GTT in WT mice 3 hours after a single injection of saline or LPS (1 mg/kg) with
571 or without IL-1Ra (10 mg/kg; n=5 per group). (**d**) *Il1r1* mRNA expression in FACS sorted islet
572 cells (n=6 experiments). (**e**) Double immunostaining of IL-1R1 and insulin in pancreatic tissue
573 sections of WT and *Il1r1*$^{-/-}$ mice. Scale bar, 50 µm. (**f**) Circulating insulin and (**g**) glucose
574 during an i.p. GTT in STZ-treated mice transplanted with WT islets or *Il1r1*$^{-/-}$ islets 18 minutes
575 after a single injection with 1 µg/kg IL-1β (n=5 and 4). *P < 0.05, **P < 0.01, ***P<0.001,
576 ****P < 0.0001. Statistical significance (P) was determined by Student's t test and in (**a-d**) by
577 ANOVA. All error bars denote s.e.m.
578
579 **Figure 5**
580 **Insulin receptor expression and activation in peritoneal macrophages**
581 (**a**) Relative mean fluorescence intensity (MFI) of insulin receptor (InsR) protein in different
582 tissue resident macrophages (4 experiments, number of circles indicates number of mice per
583 tissue). (**b**) Relative MFI of InsR protein in peritoneal macrophages from WT and DIO mice
584 (n=3 mice). (**c**) *Insr* mRNA expression in naive (M0), pro-inflammatory M1 and alternative
585 M2 polarized macrophages (n=12; 3 experiments). (**d**) A representative immunoblot of
586 insulin-induced (s473) phospho-AKT in M0, M1 and M2 polarized macrophages (1 out of 3
587 experiments). Relative phosphorylation of (**e**) AKT (ser473) and (**f**) proteins in the MAPK
588 signaling pathway (both assayed on the same samples; n=4 experiments). Gene expression

from M0 and M1 macrophages incubated with or without 1 μg/ml insulin: (**g**) *Slc2a1* (encoding GLUT1) and (**h**) *Hk2* (encoding hexokinase 2); data are expressed as fold change from untreated naive controls (n=9, 3 experiments). (**i**) Extracellular acidification rate (ECAR; mpH/min) from polarized macrophages incubated for 2 hours in the presence or absence of 1 μg/ml insulin. (n=12 or 15; 3 experiments). (**j**) ECAR measurements from M1 polarized macrophages acutely treated with or without 1 μg/ml insulin and 10 μM LY294002 or 10 μM U0126 (vertical line indicates treatment start, n=9; 3 experiments) (**k**) Glucose uptake in naive macrophages (control; n=21; 3 experiments) or incubated for 3 hours with 1 μg/ml insulin alone (n=28; 3 experiments) or in combination with 1 ng/ml IL-1β (n=15; 3 experiments). **P* < 0.05, ***P* < 0.01, ***P < 0.001, ****P < 0.0001. Statistical significance (*P*) was determined by ANOVA and in (**b, g**) by Student's t test. All error bars denote s.e.m.

Figure 6

Insulin stimulates IL-1β secretion of macrophages.

(**a**) Two-hour IL-1β secretion from 2-hour polarized macrophages isolated from WT or *Nlrp3*$^{-/-}$ mice incubated with or without 1 μg/ml insulin. (**b-d**) Two-hour IL-1β protein release from 2-hour polarized M1 macrophages with or without 1 μg/ml insulin and in combination with or without (**b**) 10 μM LY294002 or 20 μM rapamycin (n=9-12; 3 experiments), (**c**) 50 μM fasentin (n=14, 3 experiments), and (**d**) 2-deoxyglucose (2DG) or mitoTEMPO (n=6, 3 experiments): data are presented as fold stimulation from non-treated cells. (**e**) IL-1Ra and (**f**) IL-1β protein release from 16-hour polarized macrophages incubated for 12 hours with or without 1 μg/ml insulin (n=9, 3 experiments). (**g**) Circulating IL-1β levels in mice treated with or without 1 unit/kg insulin (15 minutes post injection; n=10). **P* < 0.05, ***P* < 0.01, ***P < 0.001. Statistical significance (*P*) was determined by ANOVA. All error bars denote s.e.m.

Figure 7

IL-1β shifts glucose uptake to immune cells.

In vitro glucose uptake in (**a**) macrophages incubated with or without 1 ng/ml IL-1β for 2 hours (n=15 and 11, respectively; 3 experiments) and, in (**b**) macrophages incubated with or without 1 μg /ml IL-1Ra for 3 hours (n=10 and 14, respectively; 3 experiments). (**c-g**) WT mice were injected i.p. with either saline or 1 μg/kg IL-1β or 1 μg/kg insulin (n=4 per group) 18 minutes prior to an injection of 10 μCi ^{3}H labeled 2DG. Mice were sacrificed 48 minutes after the first injection followed by assessment of glucose uptake in spleen (**c**), circulating leukocytes (**d**), visceral adipose tissue (epididymal fat pads; **e**), adipocytes isolated from epididymal fat pads (**f**) and muscle (**g**). (**h**) Number of peritoneal cells and (**i**) *ex vivo* glucose uptake in macrophages from mice injected once a day for 3 days with 35 μg/kg IL-1β (n=5 per group). (**j**) *Ex vivo* glucose uptake in peritoneal macrophages from mice acutely injected with saline or 10 mg/kg IL-1Ra. (**k**) Circulating blood glucose and insulin levels during an intra-peritoneal glucose tolerance test after treatment with 1 μg/kg IL-1β in macrophage-depleted *Rag2*$^{-/-}$ mice using an injection of 10 ml/kg clodronate or PBS liposomes (PBS; n=13, clodronate; n=8). *P < 0.05, **P < 0.01, ***P < 0.001, ****P < 0.0001. Statistical significance (P) was determined by Student's t test and in (**c-g** by ANOVA). All error bars denote s.e.m.

633 **Online methods**

634

635 **Human pancreatic islets**

636 Human islets were isolated in the islet transplantation centres of Lille and Geneva from
637 pancreata of cadaver organ donors in accordance with the local Institutional Ethical
638 Committee. They were obtained via the "islet for research distribution program" through
639 the European Consortium for Islet Transplantation, under the supervision of the Juvenile
640 Diabetes Research Foundation (31-2008-416). Islets were cultured in CMRL-1066 medium
641 containing 5 mmol/l glucose, 100 units/ml penicillin, 100 µg/ml streptomycin, 2 mM
642 Glutamax and 10 % FCS (Invitrogen) on extracellular matrix-coated 24-well plates (Novamed
643 Ltd.) in humid environment containing 5 % CO_2.

644

645 **Mouse pancreatic islets**

646 To isolate mouse islets, pancreata were perfused through the sphincter of oddi with a
647 collagenase solution (1.4 gr/l; collagenase type 4 Worthington) and digested in the same
648 solution at 37°C, followed by sequential filtration through 500 µm and 70 µm cell strainers
649 (BD). Islets were handpicked and cultured on extracellular matrix-coated 24-well plates
650 (Novamed Ltd.) in RPMI-1640 (GIBCO) containing 11.1 mM glucose, 100 units/ml penicillin,
651 100 µg/ml streptomycin, 2 mM Glutamax, 50 µg/ml gentamycin, 10 µg/ml Fungison and 10
652 % FCS. Islets were either collected directly for RNA isolation extraction or cultured for 36
653 hours on extracellular matrix-coated 24-well plates for subsequent glucose-stimulated
654 insulin secretion experiments.

655

656 **Glucose-stimulated insulin secretion assay in islets and ENDOC cells**

657 For glucose-stimulated insulin secretion experiments, islets or the human β-cell line ENDOC
658 cells (kindly provided by R. Sharfmann[51]) were cultured for 2 days and pre-incubated for 30

minutes in modified Krebs-Ringer bicarbonate buffer (KRB; 115 mM NaCl, 4.7 mM KCl, 2.6 mM $CaCl_2$ $2H_2O$, 1.2 mM KH_2PO_4, 1.2 mM $MgSO_4$ $2H_2O$, 10 mM HEPES, 0.5 % bovine serum albumin, pH 7.4) containing 2.8 mM glucose. KRB was then replaced by KRB with 2.8 mM glucose and collected after 1 hour to determine the basal insulin release. IL-1β was added at the indicated concentrations for the last 30 minutes of the 1-hour period of the basal insulin release (priming). This was followed by 1 hour in KRB with 16.7 mM glucose to determine the stimulated insulin release. The stimulatory index was defined as the ratio of insulin secretion at 16.7 mM to 2.8 mM glucose/hour and expressed as percentage of untreated control.

Animal experiments

All animal experiments were performed in mice on a C57BL/6N background unless otherwise specified. Normal mice were obtained from Charles River. For the diet induced obesity (DIO) experiments, 4 week old mice were fed a high fat diet (D12331, Research Diets; containing 58, 26 and 16 % calories from fat, carbohydrate and protein, respectively) for 20-25 weeks. Leptin receptor deficient (db/db) mice were obtained from Jackson laboratories at the age of 4 weeks and housed until the age of 16 weeks. *Irak4*$^{-/-}$ mice on a Balb/c background were kindly provided by Amgen. *IL1b*$^{-/-}$ mice mouse strains on a C57BL/6N background produced either by gene targeting[52] or with Eucomm embryonal stem cells were used. To generate the macrophage specific IL-1β knock-out mouse (*Il1b*$^{fl/fl}$*Lyz2-Cre*$^{+/-}$) chimeric mice were produced from ES cells containing a modified *Il1b* allele, which contains loxP sites flanking exons 4 and 5 and a frt-LacZ-loxP-neo-Frt cassette introduced between exon 3 and 4 (Eucomm clone HEPD0840_C04). Chimeric mice were then crossed with C57BL6/N mice and the offspring with germ line transmission of the recombined allele were crossed with Flp deleter mice[53] on Bl6/N background to excise the FRT flanked lacZ neo cassette and to obtain the *Il1b*$^{fl/fl}$ mouse. These mice were next crossed with *Lyz2-Cre* mice[54], that were previously

backcrossed to a C57BL6/N background. As littermate control mice we used the cre recombinase negative *Il1b*$^{fl/fl}$*Lyz2-Cre*$^{-/-}$ mice, and as myeloid cells specific *Il1b*$^{-/-}$ knock-out mice the *Il1b*$^{fl/fl}$*Lyz2-Cre*$^{+/-}$ mice (Supplementary Fig. 1c). *Nlrp3*$^{-/-}$ mice were generated as described previously[55]. *Rag2*$^{-/-}$ mice were bred in house. *Il1r1*$^{-/-}$ mice and immunodeficient female swiss nude were obtained from Charles River laboratories. *Glpr*$^{-/-}$/*Grp*$^{-/-}$ mice were generated as described[56].

All animal experiments were conducted according to the Swiss Veterinary Law and Institutional Guidelines and were approved by the Swiss Authorities. All animals were housed in a temperature-controlled room with a 12 h light – 12 h dark cycle and had free access to food and water.

All metabolic experiments using transgenic mice were performed with wild-type littermates as controls. The mice were between 12 and 29 weeks of age. Mice that did not gain weight in diet-induced obesity experiments were excluded. All experiments were performed at least twice with weight-matched mice and with at least a total of 4 animals per group. For drug applications (apart from antibiotics treated mice that can receive commensal bacteria from non treated controls) each cage included mice receiving all treatments in order to avoid cage dependent differences.

In vivo treatment administration

Recombinant mouse IL-1β (R&D) was injected i.p. at the indicated time and dose.

IL-1Ra (Anakinra; 10 mg/kg body weight) was injected i.p. 3 hours prior to intervention. 2-deoxyglucose (1 g per kg body weight) was injected i.p 1 hour prior to refeeding. Canagliflozin (100 mg per kg body weight) or placebo control were homogenised and orally

administered 1 hour prior to refeeding. LPS (InvivoGen; 1 mg/kg body weight) was injected i.p. at the indicated time.

Glucose tolerance tests (GTTs)

For glucose tolerance testing, mice were fasted for 6 hours starting in the morning and 2 g glucose per kg body weight was injected i.p. Blood glucose was measured using a glucometer (Freestyle; Abbott Diabetes Care Inc.).

Urine glucose levels

Glycosuria was assessed according to manufacturer's instructions (Accu Check Diabur test strips, Roche)

Fasting and refeeding experiments

Before blood collection, fasted mice were provided free access to water but not to food for 12 hours. Refed mice were treated in the same manner as the fasted mice; however, prior to blood collection, refed mice had access to food for 2 hours. In experiments done with antibiotics or with IL-1Ra injection or with *IL1b*$^{-/-}$ mice and littermate wild-type mice, blood was collected immediately before refeeding (time 0) and 2 hours after feeding. To avoid potential confounding effects due to circadian-mediated fluctuation in circulating IL-1β levels all experiments were performed at the same time of the day (between 8 to 10 am).

Glucose clamp studies

Glucose clamp studies were performed in freely moving mice as previously described[57]. Steady state glucose infusion rate was calculated once glucose infusion reached a constant rate with blood glucose levels at 5 mmol/l (70-80 minutes after the start of insulin infusion). Thereafter, blood glucose concentration was kept constant at 5 mmol/l for 15-20 minutes

and glucose infusion rate was calculated. Glucose disposal rate, and hepatic glucose production were calculated as previously described[57].

Antibiotics treatment

One week before fasting-refeeding experiment, 1 g/l antibiotic concoction consisting of vancomycin 10 mg/ml, neomycin 20 mg/ml, metronidazol 20 mg/ml (all purchased from Sigma), was administered by gavage every 12 hours. Gavage volume of 5 ml/kg body weight was delivered with a stainless steel tube. Fresh antibiotics concoction was mixed every day.

Streptozotocin induced β-cell death and Islet transplantation.

Streptozotocin (Sigma) was dissolved in citrate buffer (pH 4.5) and was i.p. injected to immunodeficient nude mice at 240 mg/kg. Only hyperglycemic mice (i.e. blood glucose > 14mM) were subjected to transplantation with 500 wild-type or *Il1r1*$^{-/-}$ mouse islets, under the kidney capsule as described in[58].

Macrophage ablation

Clodronate or PBS liposomes (ordered from ClodronateLiposomes.org) were injected i.p. (100 µl per 10 grams bodyweight) 3 days before the start of the assays. Mice were sacrificed at the end of the procedure. To verify macrophage depletion, peritoneal cells were isolated as described above and analyzed by FACS as described below. Macrophages were defined as $CD11b^+$ $F4/80^+$ double positive cells.

Primary cell isolation and culture

Cells were isolated from male C57BL/6 mice following euthanasia in a CO_2 chamber. To obtain circulating leukocytes, the heart was punctured and the collected blood was incubated briefly with red blood cells lysis buffer (154mM NH_4Cl, 10mM $KHCO_3$, 0.1mM

762 EDTA). To isolate macrophages, the peritoneum was infused with PBS containing 1% FBS and
763 the lavage was filtered through 70 μm cell strainer (BD). Kupffer cells were isolated from the
764 liver perfused with 3mL collagenase through the ductal vein followed by a 30 minute
765 incubation step and two centrifugation steps: 50 x g for 3 minutes at 4 ^{o}C, collection of the
766 upper phase and 350 x g for 5 minutes at 4^{o}C. Intestinal macrophages were isolated after
767 removal of the intestinal payer patches, cut in pieces and washed twice (20 min shaking in
768 PBS, 5mM EDTA), followed by 30min incubation in collagenase type 4 (1.4 g/l). Cells from
769 omental and epididymal fat pads were isolated after shaking with collagenase type 4 (1.4
770 g/l) for 30 min at 37^{o}C. Spleens were pushed through a 70 μm cell strainer and red cells were
771 lysed using lysis buffer (154mM NH_4CL, 10mM $KHCO_3$, 0.1mM EDTA). For islet resident
772 macrophages, handpicked pancreatic islets were dissociated by accutase (Biolegend, 50%, 2
773 minutes, 37 degrees) and washed. All cells were filtered through a 70 μm cell strainer
774 washed and resuspended in FACS buffer (PBS 0.5% BSA and 5mM EDTA). For macrophage
775 culture, cells were allowed to adhere for at least 4 hours in 48 or 96 well plates (TPP) and
776 non-adherent cells were washed away, naive macrophages were used for glucose uptake
777 assays or were polarized to M1 or M2 phenotypes as follows: 2 hours (serum free) or 16
778 hours treatment with LPS (100 ng/ml) + IFNγ (10 ng/ml) for M1 and IL-13 (10 ng/ml) + IL-4
779 (10 ng/ml) for M2 polarization, followed by 2 or 12 hours, with or without 1 μg/ml insulin in
780 the presence or absence of fasentin (50 μM; Sigma), 2-deoxyglucose (2DG; 10mM; Sigma),
781 mito-TEMPO (100 μM; Sigma), LY294002 (10 μM; Sigma), U0126 (10 μM; Sigma), rapamycin
782 (20 μM; Sigma) or followed by a 30 minute incubation with ATP (5mM; Sigma). Supernatants
783 were collected, centrifuged (at 4^{o}C, 2000 x g for 5 minutes) and stored at -80^{o}C and cells
784 were either harvested for RNA extraction (see RNA extraction and qPCR) or assayed by flow
785 cytometer for cell survival using Annexin V apoptosis detection kit (eBioscience).
786
787 **RNA extraction and qPCR**

Total RNA was extracted using the Nucleo Spin RNA II Kit (Machery Nagel) or using RNeasy Lipid Tissue (QIAGEN). RNA concentrations were normalized and cDNA was prepared with random hexamers (Microsynth) and Superscript II (Invitrogen) according to the instructions of the supplier. RNA expression was determined with TaqMan assays and the real time PCR system 7500 (Applied Biosystems). The following TaqMan assays were used:

Mouse: *Gadph*: Mm99999915_g1, *Actb*: Mm00607939_s1, *Slc2a1* (encoding GLUT1): Mm00441480_m1. *Il1b*: Mm0043228_m1, *InsR*: Mm01211875_m1, *Cxcl1*: Mm04207460_m1, *Hk2*: Mm00443395_m1, *Il1a*: Mm00439621_m1, *Il1r1*: Mm00434237_m1, *Ccl2*: Mm00441242_m1, *Tnf*: Mm00443258_m1, *Il6*: Mm004461920_m1. Data were normalized with the geometrical mean of *Gadph* and *Actb* for macrophage mRNA and quantified using the comparative $2^{-\Delta\Delta CT}$ method.

Protein and protein-phosphorylation measurement assays

Insulin concentrations were determined using human insulin ultrasensitive ELISAs (Mercodia) or mouse/rat insulin kits (Mesoscale Discovery). Mouse active GLP-1 was assayed using a Mesoscale discovery kit. Protein phosphorylation was assayed using whole cell lysates (10 µg total protein) and Mesoscale Discovery kinase phosphorylation assay kits (AKT signalling panel; K15177D and MAP kinase panel; K15101D) according to manufacturer's instructions. Mouse cytokine concentrations were assayed using the V-plex mouse IL-1β TNFα, IL-6, and CXCL1 kit from Mesoscale Discovery with the following modifications: for circulating cytokine assay, after withdrawal, blood was incubated for 30 minutes at room temperature and sera were collected after 20 minutes of centrifugation (4°C, 2000 x g). Samples were incubated in the assay plate overnight at 4°C with gentle shaking. IL-1Ra was determined using ELISA assays (R&D).

Glucose bio-distribution assay

814 Male C57BL/6 mice were fasted for 3 hours in the morning, i.p. injected with IL-1β (1 μg/kg
815 body weight) or saline and 18 minutes later with ^{3}H labeled 2-deoxy glucose (10 μCi per
816 mouse, Perkin Elmer). After 30 minutes mice were sacrificed, quadriceps muscle, epididymal
817 adipose tissue and spleen were weighed, washed immediately in ice cold PBS and incubated
818 with lysis buffer (10% glycerol, 5% 2-mercaptoethanol, 2.3% SDS, 62.5mM Tris pH6.8, 6M
819 urea) followed by sonication. Leukocytes were isolated as described above, washed twice
820 with ice cold PBS, counted and lysed with 0.1% SDS. Triplicate samples were then measured
821 in a beta counter. Data are presented for organs as percentage beta counts per minute per
822 mg tissue and as beta counts per cell for Leukocytes. In experiments with refed mice,
823 fluorescent 2-deoxyglucose (2NBDG 500nmole per mouse; Invitrogen) was i.p. injected
824 immediately after a refeeding window. Mice were sacrificed 1 hour later, peritoneal cells
825 were harvested and analyzed by flow cytometer (BD Acurri).
826
827 ***In vitro* glucose uptake assay**
828 For *in vitro* treatment, macrophages were pre-incubated for 2 hours with KRB containing 1
829 mM glucose (as described in GSIS section) with or without the indicated treatment. To
830 determine glucose uptake, macrophages were then incubated for 30 minutes with 0.4 nCi ^{3}H
831 labeled 2-deoxy glucose (Perkin Elmer), washed twice with ice cold PBS, lysed with 0.1 % SDS
832 and transferred into scintillation fluid. ^{3}H labeled 2-deoxy glucose uptake was measured in a
833 beta counter.
834
835 **Immunoblotting**
836 We separated proteins (8-12 μg) in 4-12 % NuPAGE gels (Invitrogen), blotted them onto
837 nitrocellulose membranes (Bio-Rad) and incubated them with antibodies against total AKT
838 (pan AKT; #4691), pAKT (s473; #9271) and Insulin receptor β (4B8; #3025.) All antibodies

were purchased from Cell Signaling. Blots were analyzed using image lab 4.1 software (Bio-Rad).

Flow cytometry

To obtain single cells, islets were dispersed with trypsin (Invitrogen) for 6 minutes at 37°C, washed with PBS, centrifuged at 300 x g, 5 minutes, 4°C and resuspended in FACS buffer (PBS with 0.5% BSA and 2 mM EDTA). After 15 minutes incubation with an Fc blocker (Anti-mouse CD16/CD32; eBioscience 14-0161) peritoneal cells or single islet cells were stained with the appropriate antibodies for 30 minutes at 4°C in the dark. To verify the effect of the clodronate depletion, cells from $Rag^{-/-}$ mice were stained with anti F4/80 (clone BM8) and anti CD11b (clone M1/70). To determine the peritoneal cell composition, cells were stained with anti CD3e (clone 145-2C11), anti GR-1 (clone RB6-8C5), anti CD11b (clone M1/70), anti F4/80- (clone BM8), anti CD19 (clone RA3-6B2) and anti Siglec-F-APC (clone E50-2440). Single cells from adipose tissue, islets, Liver, small intestine, and colon were stained with CD45 (clone 30-F11) for immune cells (antibodies were purchased from eBioscience, Siglec-F was purchased from BD Pharmingen). For additional intra-cellular Insulin receptor intensity in tissue resident macrophages, cells were also incubated with intracellular fixation buffer (eBioscience) following incubation with permeabilization buffer (eBioscience) according to manufacturer's instructions. Anti InsR β (Cell Signaling; 3025S) was added following secondary conjugated donkey anti rabbit antibody (Invitrogen). Stained cells were washed twice with FACS buffer prior to FACS acquisition. Cells were analyzed with an Accuri C6 flow cytometer or LSR-Fortessa (BD Bioscience). Dispersed islet cells were analyzed and sorted with a FACS ARIA III cell sorter (BD Biosciences) using FACS Diva software (BD Biosciences). All samples were stained with appropriate isotype control antibodies; viability staining was done using 7-AAD (Sigma) or DAPI (Biolegend). Macrophages were defined as $CD11b^{+}$ $F4/80^{+}$ double positive cells. Data were analyzed using Flow Jo 9.4 software (Tree Star).

865

866 **Extracellular acidification measurements**

867 An XF24 or an XF96e Extracellular Flux analyzer (Seahorse Biosciences) was used to
868 determine the bioenergetic profile of FACS sorted macrophages (F4/80 and CD11b double
869 positive peritoneal cells). Cells were plated at a density of 500'000 or 300'000 cells per well
870 in XF24 or XF96 plate accordingly, incubated for 4 hours and washed before being
871 stimulated with LPS (100 ng/ml) + IFNγ (10 ng/ml) or IL-4\IL-13 (10 ng/ml) for the indicated
872 times. Insulin was injected or added to the media (1 μg/ml end concentration) for the
873 indicated time. Prior to the assay, cells were incubated in unbuffered RPMI (Seahorse
874 Biosciences) containing 11.1 mM glucose for 1 hour. Then extracellular acidification rate
875 were assessed during 2 minutes. Basal measurements were followed by measurements
876 upon injection of the following agents: Glucose (26.8 mM), oligomycin (1 μM),
877 carbonilcyanide p-triflouromethoxyphenylhydrazone (FCCP) (2 μM), rotenone (1 μM), and 2-
878 deoxyglucose (2DG; 10mM). To activate cells with insulin during Seahorse measurments cells
879 were incubated in unbuffered RPMI containing 5mM glucose for 1 hour, then extracellular
880 acidification rate were assessed during 2 minutes for 6 basal measurements followed by
881 injections of inhibitors (LY294002, 10 μM; U0126, 10 μM) or DMSO as control and insulin (1
882 μg/ml). Oligomycin, FCCP, and rotenone were purchased from Sigma.

883

884 **Immunofluorescence staining**

885 Pancreata were fixed overnight in 4% paraformaldehyde at 4^{o}C, followed by paraffin
886 embedding. Sections were deparaffinized, re-hydrated and incubated 1 hour at room
887 temperature with guinea pig anti-insulin antibody (Dako; A0564), followed by detection with
888 a fluorescein-conjugated donkey anti-guinea pig antibody (Dako). Subsequently, the sections
889 were labeled for IL-1R1 with goat anti IL-1-R1 antibody (R&D; AF771), followed by detection
890 with a fluorescein-conjugated donkey anti-goat antibody (Invitrogen).

Statistics

Appropriate statistical tests were performed where required. Comparisons between groups were performed using unpaired, two-sided *t*-test for normally distributed data. For grouped comparisons, one-way ANOVA or two-way ANOVA followed by Sidak's multiple comparisons analysis were used where appropriate. Statistically significant outliers were assessed using ROUT's test (O = 1%) and were excluded from analysis. Data analysis was performed using GraphPad Prism v7.0a Software Excluding diet induced obesity experiments, all animal studies were performed on weight matched mice. There was no other prior randomization or blinding. Data are expressed as means ± s.e.m. and statistical significance is denoted as $*P < 0.05$, $**P < 0.01$, $***P < 0.001$ and, $****P < 0.0001$. n numbers indicate biological replicates for *in vitro* experiments or number of mice for *in vivo* experiments.

Method-only references

51. Ravassard, P*., et al.* A genetically engineered human pancreatic beta cell line exhibiting glucose-inducible insulin secretion. *The Journal of clinical investigation* **121**, 3589-3597 (2011).

52. Horai, R*., et al.* Production of mice deficient in genes for interleukin (IL)-1alpha, IL-1beta, IL-1alpha/beta, and IL-1 receptor antagonist shows that IL-1beta is crucial in turpentine-induced fever development and glucocorticoid secretion. *The Journal of experimental medicine* **187**, 1463-1475 (1998).

53. Farley, F.W., Soriano, P., Steffen, L.S. & Dymecki, S.M. Widespread recombinase expression using FLPeR (flipper) mice. *Genesis* **28**, 106-110 (2000).

54. Clausen, B.E., Burkhardt, C., Reith, W., Renkawitz, R. & Forster, I. Conditional gene targeting in macrophages and granulocytes using LysMcre mice. *Transgenic research* **8**, 265-277 (1999).

55. Martinon, F., Petrilli, V., Mayor, A., Tardivel, A. & Tschopp, J. Gout-associated uric acid crystals activate the NALP3 inflammasome. *Nature* **440**, 237-241 (2006).

56. Preitner, F*., et al.* Gluco-incretins control insulin secretion at multiple levels as revealed in mice lacking GLP-1 and GIP receptors. *The Journal of clinical investigation* **113**, 635-645 (2004).

57. Wueest, S*., et al.* Fas (CD95) expression in myeloid cells promotes obesity-induced muscle insulin resistance. *EMBO molecular medicine* **6**, 43-56 (2014).

58. Caiazzo, R*., et al.* Quantitative in vivo islet potency assay in normoglycemic nude mice correlates with primary graft function after clinical transplantation. *Transplantation* **86**, 360-363 (2008).

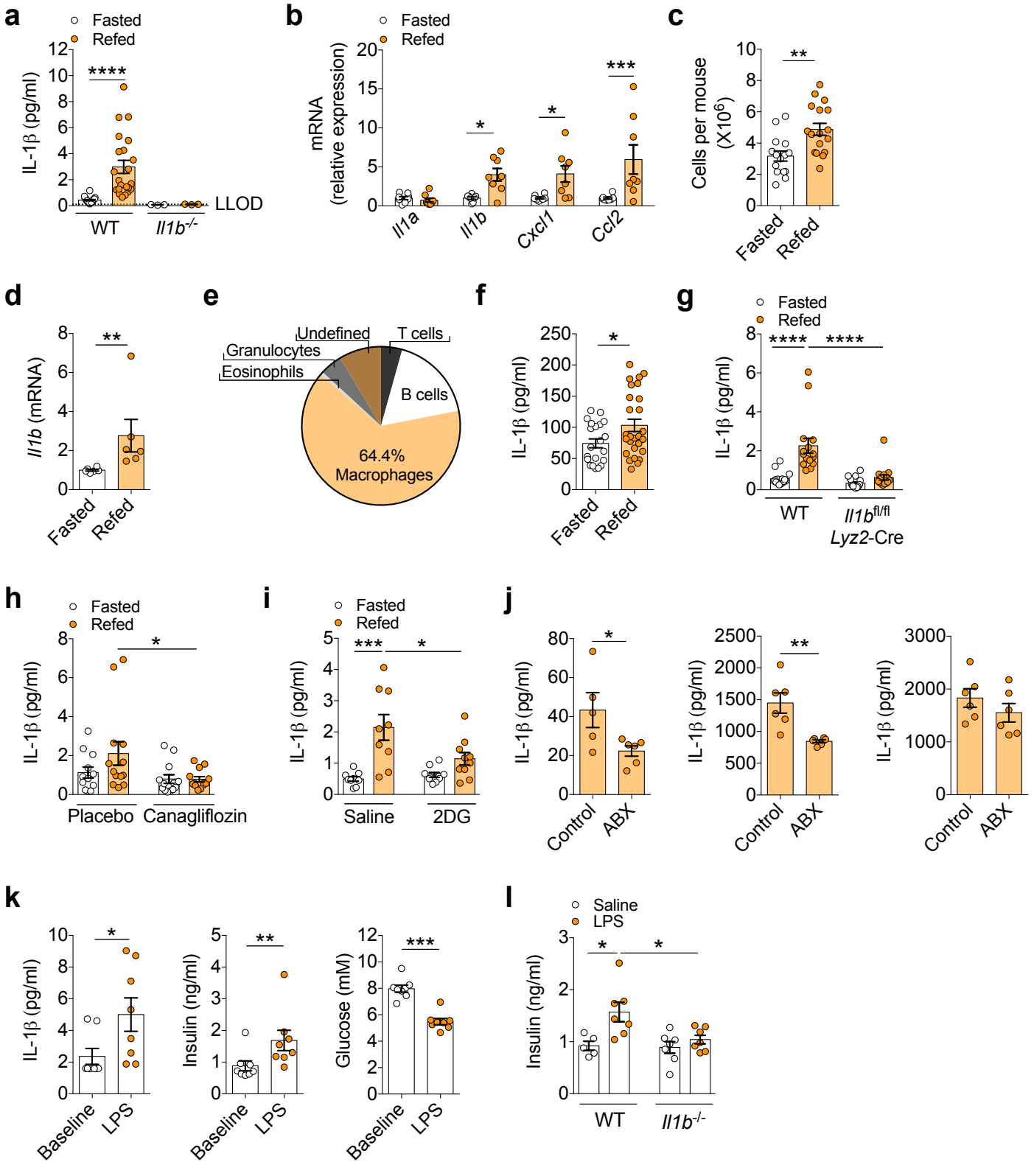
a
Fasted
Refed
IL-1β (pg/ml)
****
LLOD
WT
Il1b-/-
b
Fasted
Refed
mRNA (relative expression)
*
*
***
Il1a
Il1b
Cxcl1
Ccl2
c
Cells per mouse (X10^6)
**
Fasted
Refed
d
Il1b (mRNA)
**
Fasted
Refed
e
Undefined
T cells
Granulocytes
Eosinophils
B cells
64.4%
Macrophages
f
IL-1β (pg/ml)
*
Fasted
Refed
g
Fasted
Refed
IL-1β (pg/ml)
****
****
WT
Il1bfl/fl
Lyz2-Cre
h
Fasted
Refed
IL-1β (pg/ml)
*
Placebo
Canagliflozin
i
Fasted
Refed
IL-1β (pg/ml)
***
*
Saline
2DG
j
IL-1β (pg/ml)
*
Control
ABX
IL-1β (pg/ml)
**
Control
ABX
IL-1β (pg/ml)
Control
ABX
k
IL-1β (pg/ml)
*
Baseline
LPS
Insulin (ng/ml)
**
Baseline
LPS
Glucose (mM)
***
Baseline
LPS
l
Saline
LPS
Insulin (ng/ml)
*
*
WT
Il1b-/-

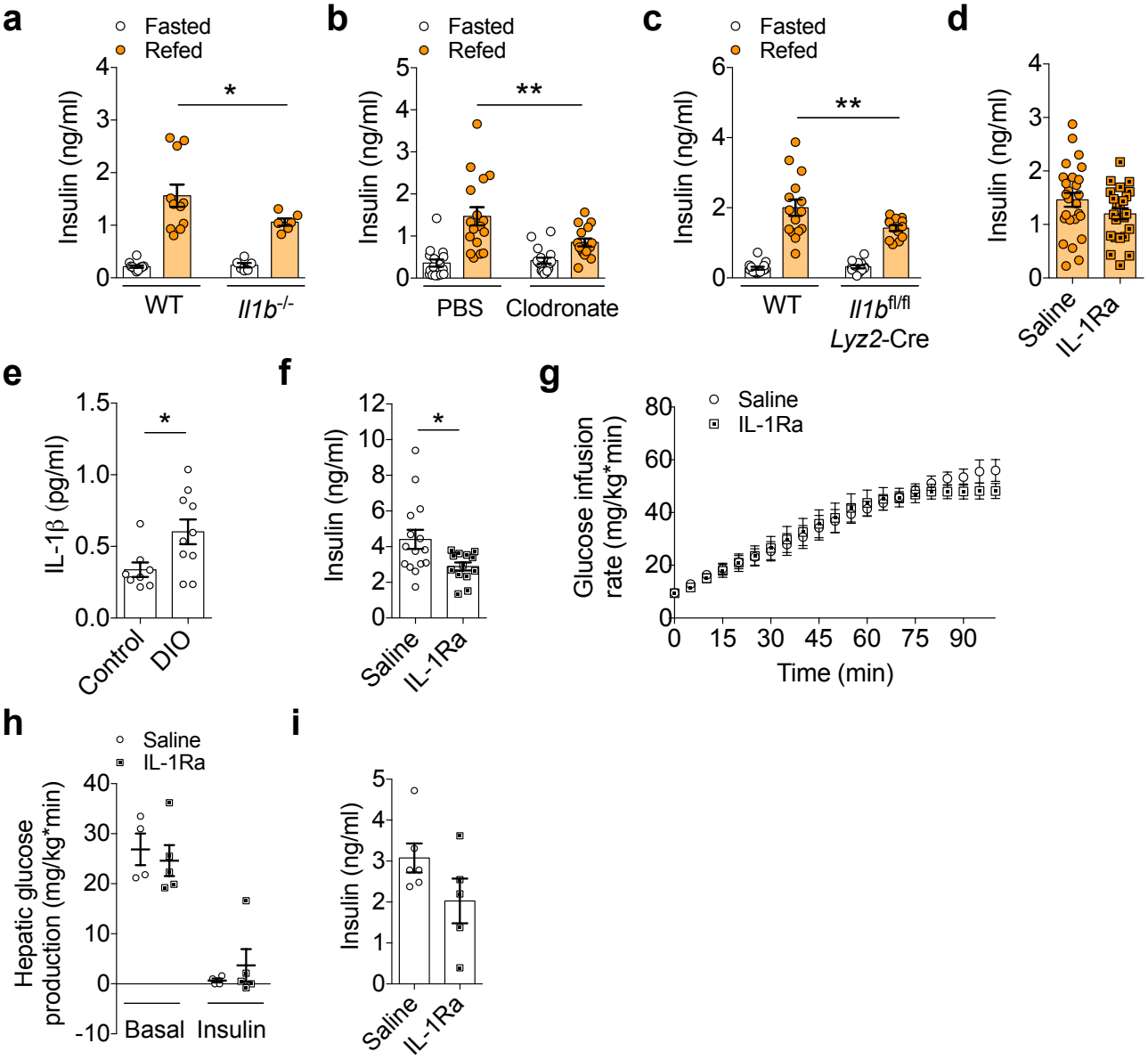
a
Fasted
Refed
Insulin (ng/ml)
*
WT
Il1b-/-
b
Fasted
Refed
Insulin (ng/ml)
**
PBS
Clodronate
c
Fasted
Refed
Insulin (ng/ml)
**
WT
Il1bfl/fl
Lyz2-Cre
d
Insulin (ng/ml)
Saline
IL-1Ra
e
IL-1β (pg/ml)
*
Control
DIO
f
Insulin (ng/ml)
*
Saline
IL-1Ra
g
Saline
IL-1Ra
Glucose infusion rate (mg/kg*min)
Time (min)
h
Saline
IL-1Ra
Hepatic glucose production (mg/kg*min)
Basal
Insulin
i
Insulin (ng/ml)
Saline
IL-1Ra

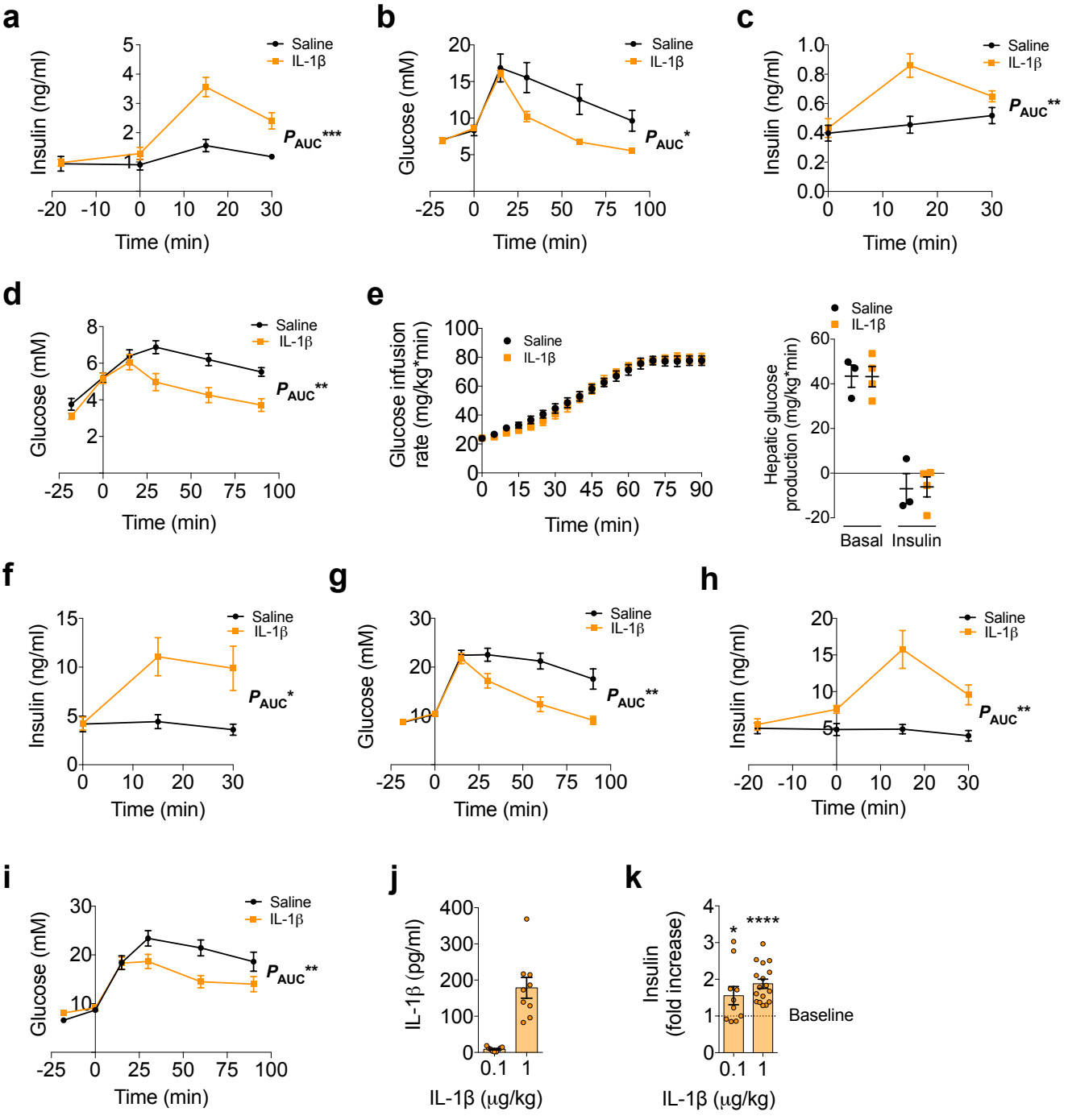
a
Insulin (ng/ml)
Saline
IL-1β
P_{AUC}***
Time (min)
b
Glucose (mM)
P_{AUC}*
c
P_{AUC}**
d
P_{AUC}**
e
Glucose infusion rate (mg/kg*min)
Hepatic glucose production (mg/kg*min)
Basal
Insulin
f
P_{AUC}*
g
P_{AUC}**
h
P_{AUC}**
i
P_{AUC}**
j
IL-1β (pg/ml)
IL-1β (μg/kg)
k
Insulin (fold increase)
Baseline

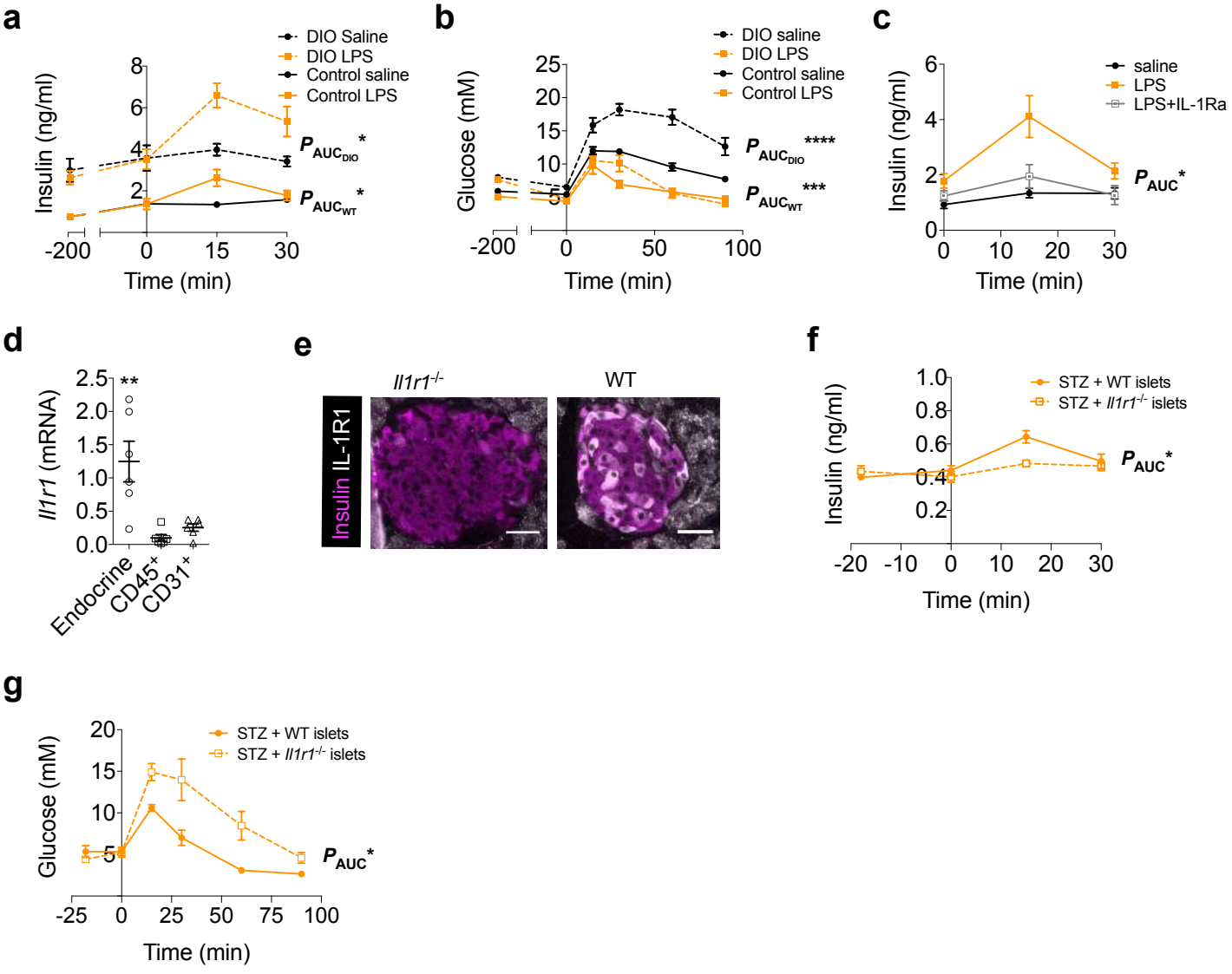
a
DIO Saline
DIO LPS
Control saline
Control LPS
Insulin (ng/ml)
Time (min)
$P_{AUC_{DIO}}$ *
$P_{AUC_{WT}}$ *
b
DIO saline
DIO LPS
Control saline
Control LPS
Glucose (mM)
Time (min)
$P_{AUC_{DIO}}$ ****
$P_{AUC_{WT}}$ ***
c
saline
LPS
LPS+IL-1Ra
Insulin (ng/ml)
Time (min)
P_{AUC} *
d
Il1r1 (mRNA)
**
Endocrine
CD45+
CD31+
e
Il1r1-/-
WT
Insulin IL-1R1
f
STZ + WT islets
STZ + Il1r1-/- islets
Insulin (ng/ml)
Time (min)
P_{AUC} *
g
STZ + WT islets
STZ + Il1r1-/- islets
Glucose (mM)
Time (min)
P_{AUC} *

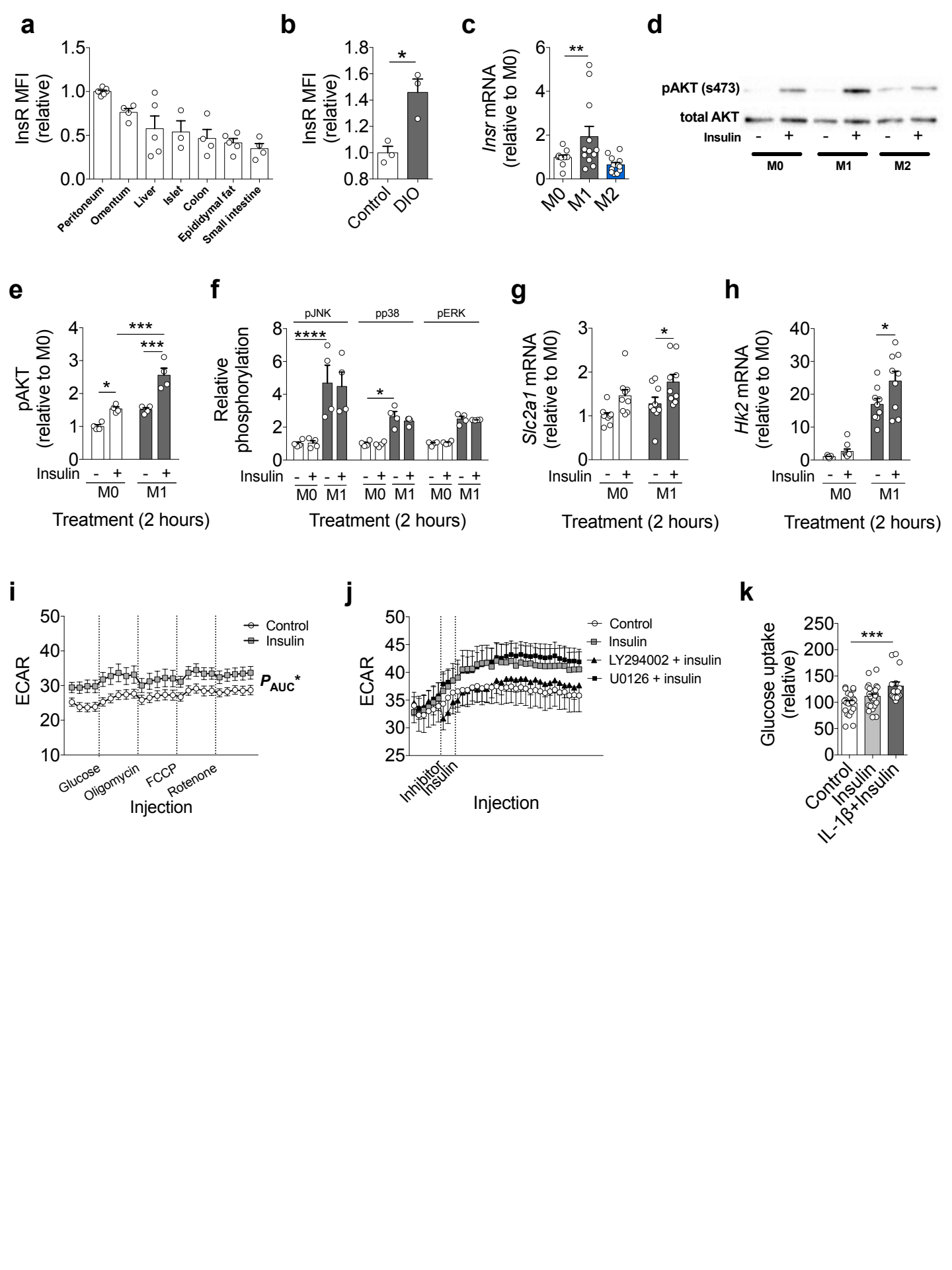
a
InsR MFI (relative)
1.5
1.0
0.5
0.0
Peritoneum
Omentum
Liver
Islet
Colon
Epididymal fat
Small intestine
b
InsR MFI (relative)
1.8
1.6
1.4
1.2
1.0
0.8
*
Control
DIO
c
Insr mRNA (relative to M0)
6
4
2
0
**
M0
M1
M2
d
pAKT (s473)
total AKT
Insulin - + - + - +
M0
M1
M2
e
pAKT (relative to M0)
4
3
2
1
0
***
***
*
Insulin - + - +
M0
M1
Treatment (2 hours)
f
Relative phosphorylation
8
6
4
2
0
pJNK
pp38
pERK
****
*
Insulin - + - + - + - + - + - +
M0
M1
M0
M1
M0
M1
Treatment (2 hours)
g
Slc2a1 mRNA (relative to M0)
3
2
1
0
*
Insulin - + - +
M0
M1
Treatment (2 hours)
h
Hk2 mRNA (relative to M0)
40
30
20
10
0
*
Insulin - + - +
M0
M1
Treatment (2 hours)
i
ECAR
50
40
30
20
10
Control
Insulin
P AUC *
Glucose
Oligomycin
FCCP
Rotenone
Injection
j
ECAR
50
45
40
35
30
25
Control
Insulin
LY294002 + insulin
U0126 + insulin
Inhibitor
Insulin
Injection
k
Glucose uptake (relative)
250
200
150
100
50
0
***
Control
Insulin
IL-1β+Insulin

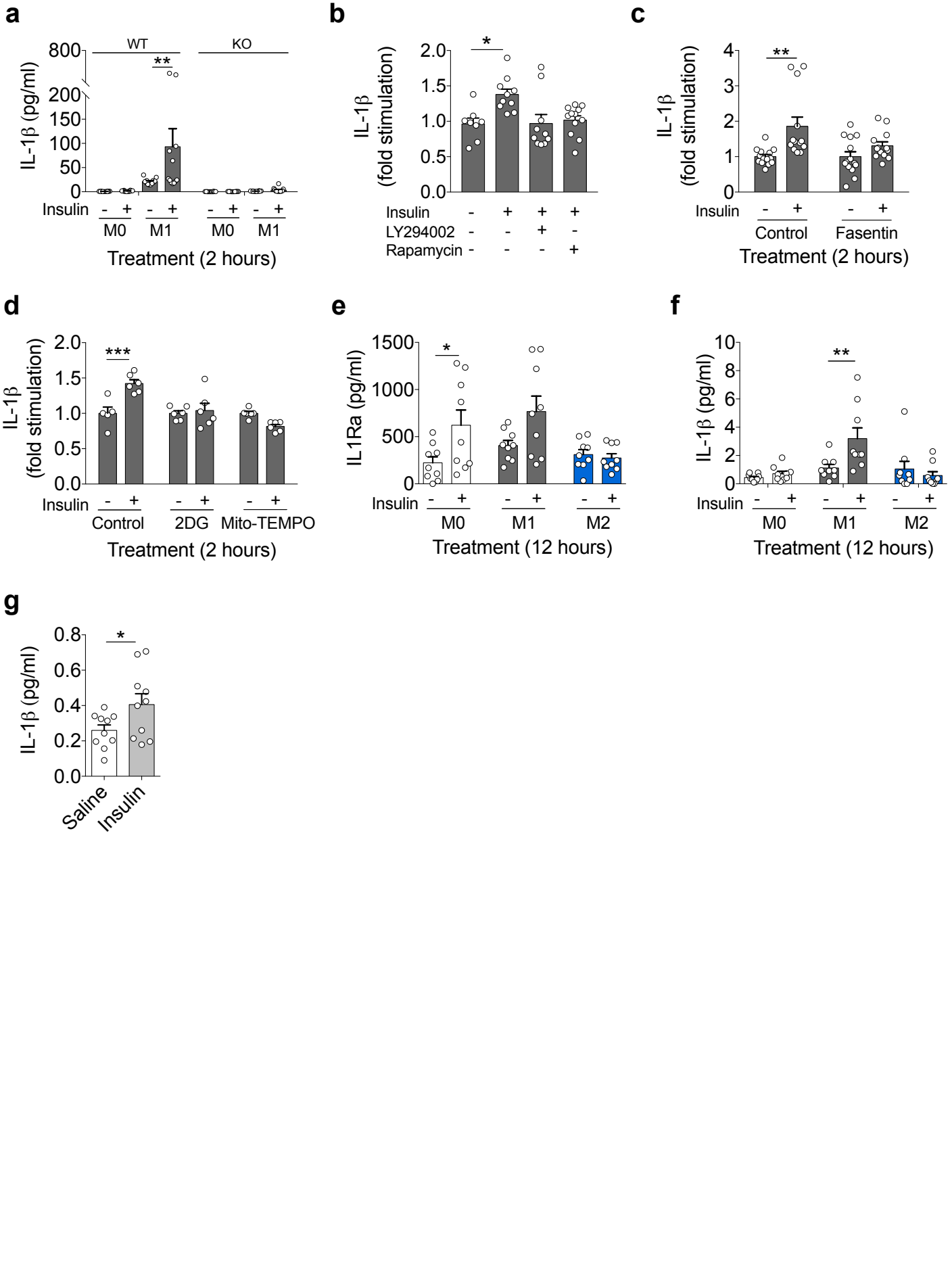
a
WT
KO
**
800
200
150
100
50
0
IL-1β (pg/ml)
Insulin - + - + - + - +
M0 M1 M0 M1
Treatment (2 hours)
b
*
2.0
1.5
1.0
0.5
0.0
IL-1β (fold stimulation)
Insulin - + + +
LY294002 - - + -
Rapamycin - - - +
c
**
4
3
2
1
0
IL-1β (fold stimulation)
Insulin - + - +
Control Fasentin
Treatment (2 hours)
d
***
2.0
1.5
1.0
0.5
0.0
IL-1β (fold stimulation)
Insulin - + - + - +
Control 2DG Mito-TEMPO
Treatment (2 hours)
e
*
1500
1000
500
0
IL1Ra (pg/ml)
Insulin - + - + - +
M0 M1 M2
Treatment (12 hours)
f
**
10
8
6
4
2
0
IL-1β (pg/ml)
Insulin - + - + - +
M0 M1 M2
Treatment (12 hours)
g
*
0.8
0.6
0.4
0.2
0.0
IL-1β (pg/ml)
Saline
Insulin

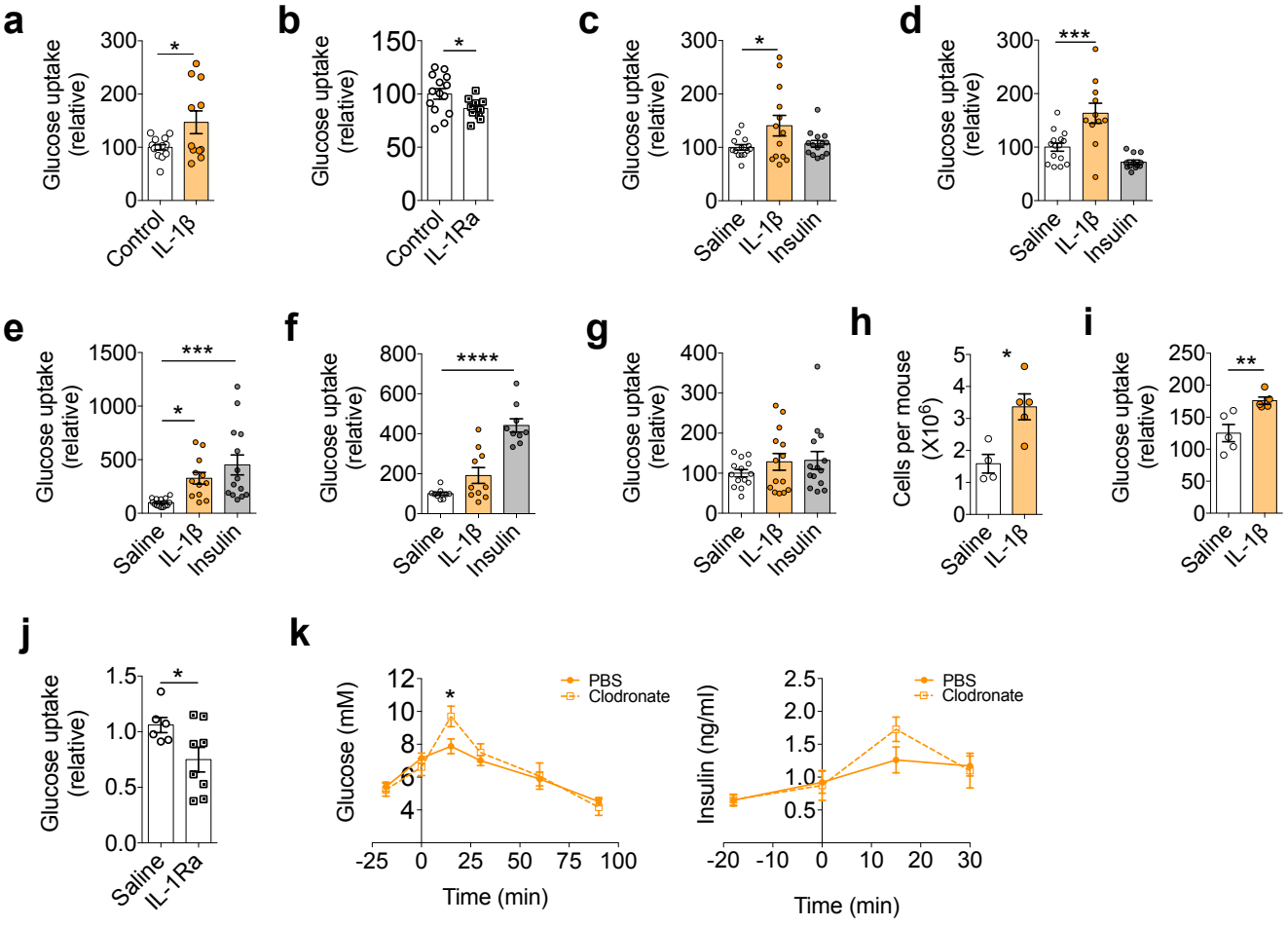
a
Glucose uptake (relative)
300
200
100
0
*
Control
IL-1β
b
Glucose uptake (relative)
150
100
50
0
*
Control
IL-1Ra
c
Glucose uptake (relative)
300
200
100
0
*
Saline
IL-1β
Insulin
d
Glucose uptake (relative)
300
200
100
0
***
Saline
IL-1β
Insulin
e
Glucose uptake (relative)
1500
1000
500
0
***
*
Saline
IL-1β
Insulin
f
Glucose uptake (relative)
800
600
400
200
0
****
Saline
IL-1β
Insulin
g
Glucose uptake (relative)
400
300
200
100
0
Saline
IL-1β
Insulin
h
Cells per mouse (X10^6)
5
4
3
2
1
0
*
Saline
IL-1β
i
Glucose uptake (relative)
250
200
150
100
50
0
**
Saline
IL-1β
j
Glucose uptake (relative)
1.5
1.0
0.5
0.0
*
Saline
IL-1Ra
k
Glucose (mM)
12
10
8
6
4
*
PBS
Clodronate
-25
0
25
50
75
100
Time (min)
Insulin (ng/ml)
2.5
2.0
1.5
1.0
0.5
PBS
Clodronate
-20
-10
0
10
20
30
Time (min)

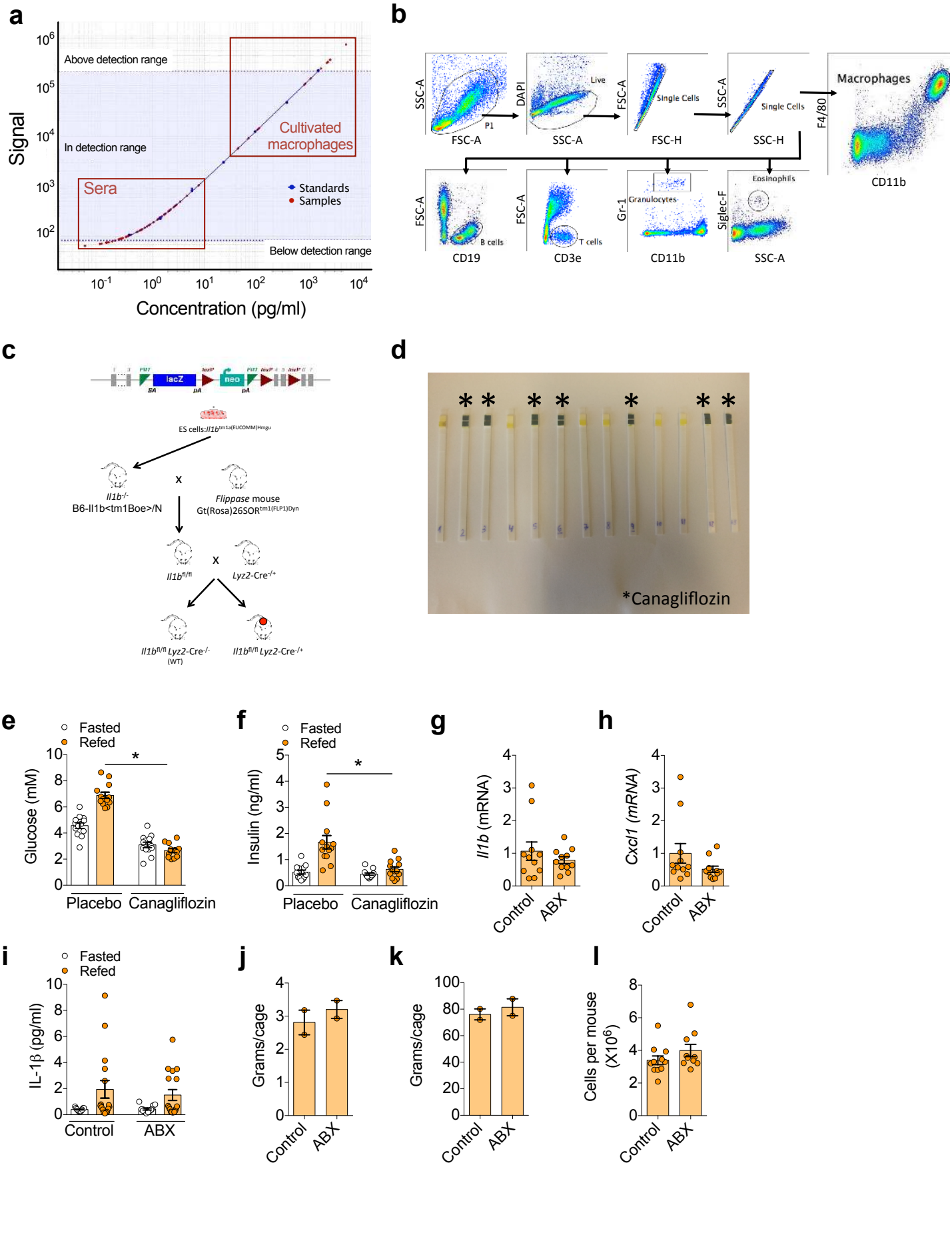
a
Above detection range
In detection range
Below detection range
Cultivated macrophages
Sera
Standards
Samples
Signal
Concentration (pg/ml)
b
SSC-A
FSC-A
P1
DAPI
Live
FSC-H
Single Cells
SSC-H
F4/80
Macrophages
CD11b
CD19
B cells
CD3e
T cells
Gr-1
Granulocytes
Siglec-F
Eosinophils
c
lacZ
neo
ES cells:Il1b tm1a(EUCOMM)Hmgu
Il1b-/-
B6-Il1b<tm1Boe>/N
Flippase mouse
Gt(Rosa)26SOR tm1(FLP1)Dyn
Il1bfl/fl
Lyz2-Cre-/+
Il1bfl/fl Lyz2-Cre-/-
(WT)
Il1bfl/fl Lyz2-Cre-/+
d
*Canagliflozin
e
Fasted
Refed
Glucose (mM)
Placebo
Canagliflozin
f
Insulin (ng/ml)
g
Il1b (mRNA)
Control
ABX
h
Cxcl1 (mRNA)
i
IL-1β (pg/ml)
j
Grams/cage
k
Grams/cage
l
Cells per mouse (X10^6)

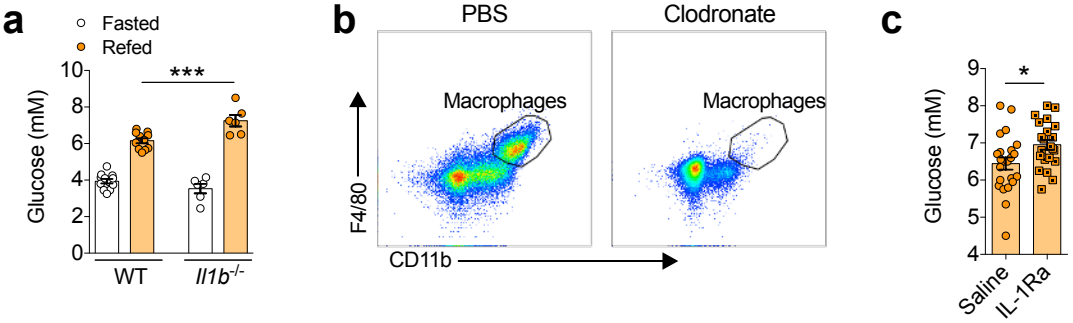
a
Fasted
Refed
Glucose (mM)
10
8
6
4
2
0
***
WT
Il1b-/-
b
PBS
Clodronate
Macrophages
Macrophages
F4/80
CD11b
c
Glucose (mM)
9
8
7
6
5
4
*
Saline
IL-1Ra

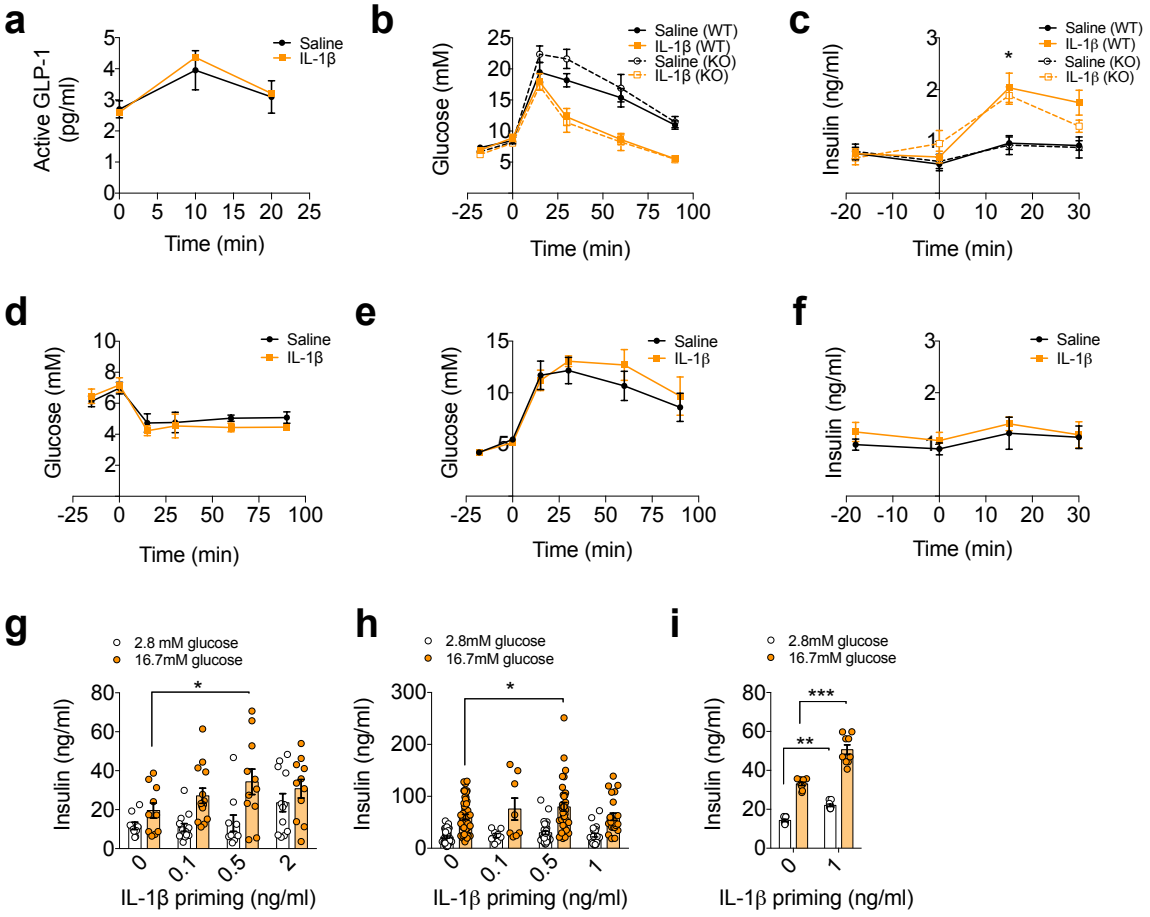
a
Active GLP-1 (pg/ml)
Saline
IL-1β
Time (min)
b
Glucose (mM)
Saline (WT)
IL-1β (WT)
Saline (KO)
IL-1β (KO)
Time (min)
c
Insulin (ng/ml)
Saline (WT)
IL-1β (WT)
Saline (KO)
IL-1β (KO)
Time (min)
d
Glucose (mM)
Saline
IL-1β
Time (min)
e
Glucose (mM)
Saline
IL-1β
Time (min)
f
Insulin (ng/ml)
Saline
IL-1β
Time (min)
g
2.8 mM glucose
16.7mM glucose
Insulin (ng/ml)
IL-1β priming (ng/ml)
h
2.8mM glucose
16.7mM glucose
Insulin (ng/ml)
IL-1β priming (ng/ml)
i
2.8mM glucose
16.7mM glucose
Insulin (ng/ml)
IL-1β priming (ng/ml)

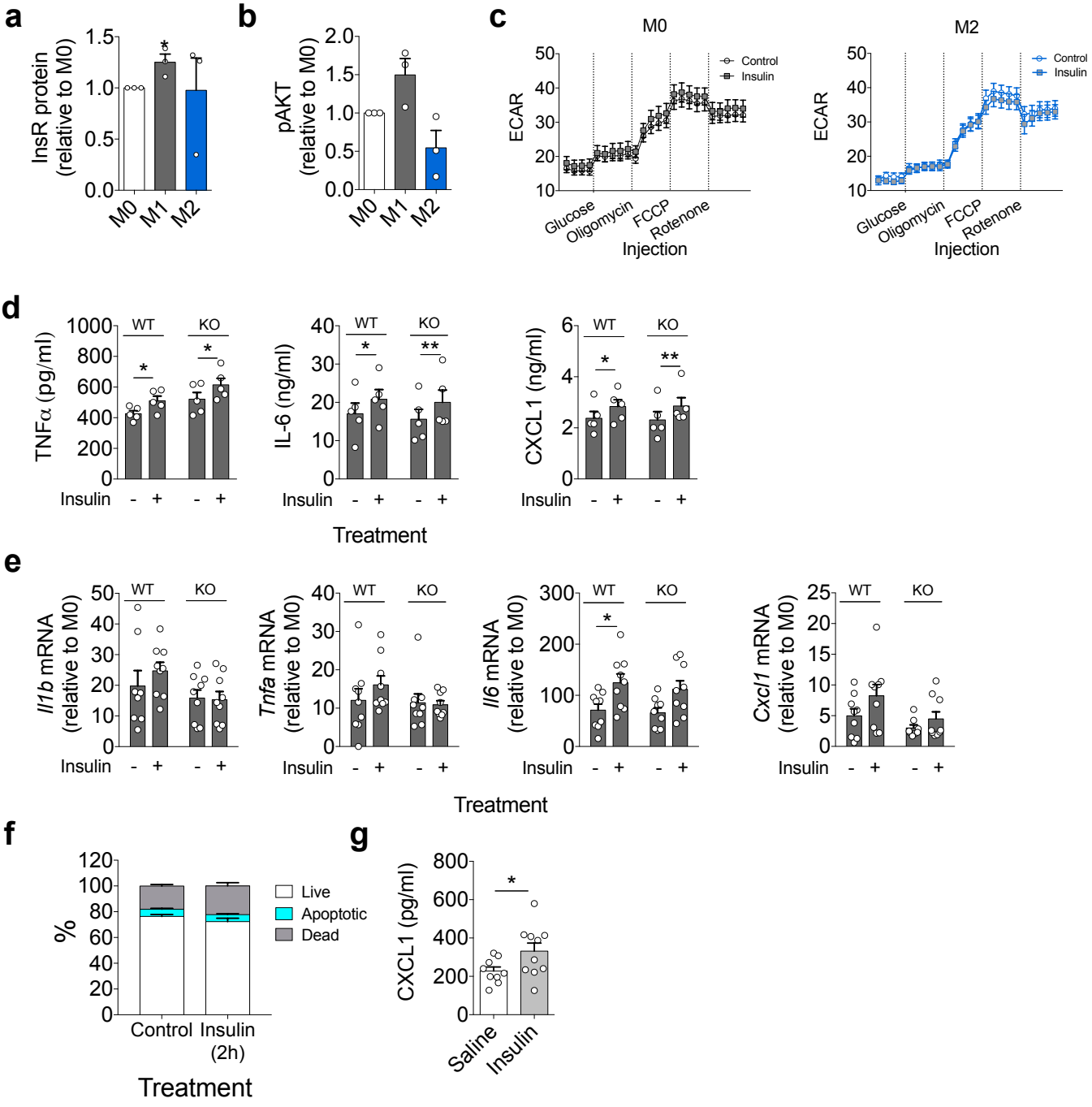
a
InsR protein (relative to M0)
M0
M1
M2
b
pAKT (relative to M0)
c
M0
M2
ECAR
Control
Insulin
Glucose
Oligomycin
FCCP
Rotenone
Injection
d
TNFα (pg/ml)
IL-6 (ng/ml)
CXCL1 (ng/ml)
WT
KO
Insulin
Treatment
e
Il1b mRNA (relative to M0)
Tnfa mRNA (relative to M0)
Il6 mRNA (relative to M0)
Cxcl1 mRNA (relative to M0)
f
%
Live
Apoptotic
Dead
Control
Insulin (2h)
Treatment
g
CXCL1 (pg/ml)
Saline
Insulin

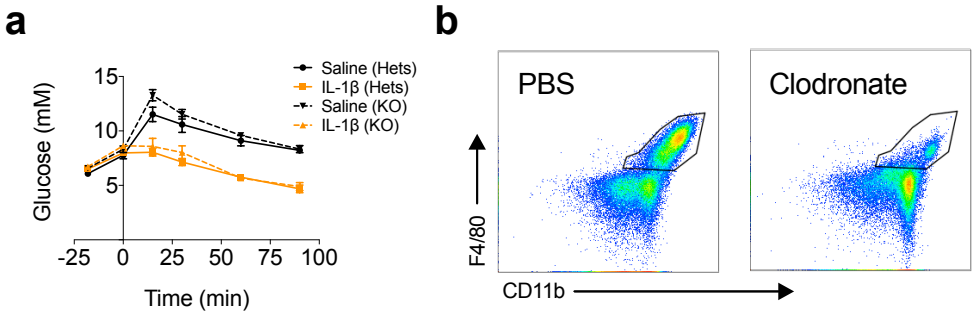
a
Glucose (mM)
15
10
5
-25
0
25
50
75
100
Time (min)
Saline (Hets)
IL-1β (Hets)
Saline (KO)
IL-1β (KO)
b
PBS
Clodronate
F4/80
CD11b

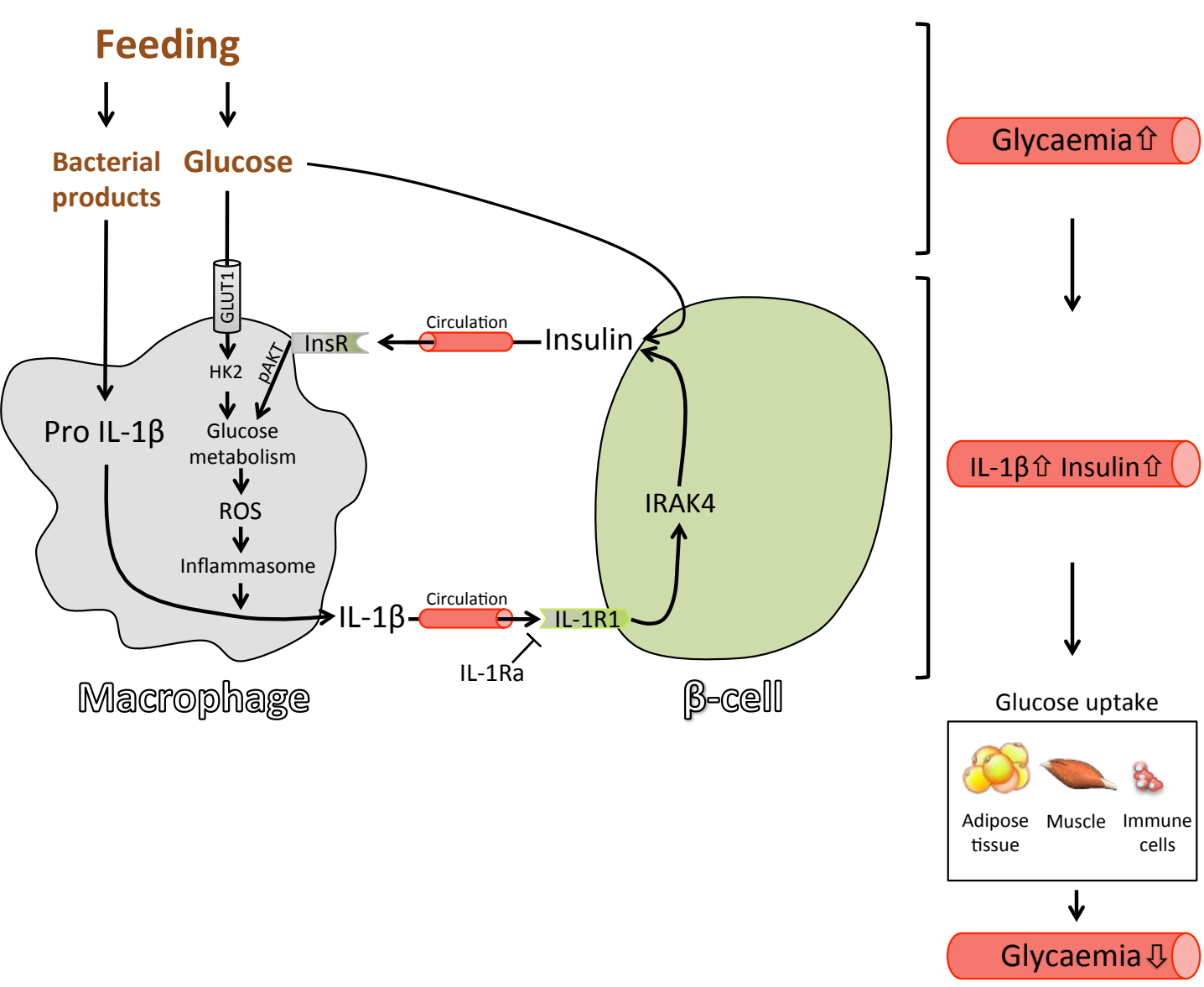
Feeding
Bacterial products
Glucose
GLUT1
HK2
pAKT
InsR
Circulation
Insulin
Pro IL-1β
Glucose metabolism
ROS
Inflammasome
IL-1β
Circulation
IL-1R1
IL-1Ra
IRAK4
Macrophage
β-cell
Glycaemia⇧
IL-1β⇧ Insulin⇧
Glucose uptake
Adipose tissue
Muscle
Immune cells
Glycaemia⇩